Elsevier Editorial System(tm) for Lithos
Manuscript Draft

Manuscript Number:

Title: Mantle Xenoliths from intracratonic Eastern Paraguay (South America Platform) and Andean Domain: a comparison

Article Type: Special Issue: Lithospheric Mantle

Keywords: Intra-plate magmatism; Sub-arc mantle; Andes, Eastern Paraguay, mantle xenoliths, clinopyroxenes, mantle metasomatism.

Corresponding Author: Prof. Piero Comin-Chiaramonti, Dr

Corresponding Author's Institution: Trieste University

First Author: Piero Comin-Chiaramonti, Prof

Order of Authors: Piero Comin-Chiaramonti, Prof; Friedrich Lucassen, Dr; Angelo De Min, Dr; Celso B Gomes, Prof

Abstract: Protogranular spinel-peridotite mantle xenoliths and host sodic alkaline lavas of Cretaceous to Paleogene age from ≈ 26°S, central eastern Paraguay and Andes are studied for: (1) trace element behaviour; (2) Sr-Nd-Pb relationships among host lavas, mantle xenoliths and hosted pyroxenes. The mantle xenoliths are distinct into two main suites, i.e. LK (relatively low in K and incompatible elements, IE) and HK (high in K and IE), both ranging from lherzolite to dunite and showing trends of "melt extraction". The hosted clinopyroxenes display extremely variable enrichment/depletion behaviours, mainly LREE. The enriched components were mostly trapped in clinopyroxenes that previously crystallized from depleted to quasi-chondritic mantle sources. Oxygen isotopes (clinopyroxene-olivine pairs) suggest equilibration temperatures higher in the HK suite than in LK suite.
Sr-Nd-Pb isotope ratios of alkaline mafic intra-plate magmatism constrain the isotopic compositions of the lithospheric mantle. Most small-volume sodic lavas were derived from a depleted lithospheric mantle source with rather uniform initial 143Nd/144Nd (0.5127-0.5128) and 87Sr/86Sr (0.7032-0.7040). The initial 206Pb/204Pb ratios are variable (18.5-19.7) at uniform 207Pb/204Pb ratios (15.60±0.05). The variable Sr ,

Nd and Pb ratios are different from depleted mantle (DM), enriched (EM), or high-μ (HIMU) mantle reservoirs and probably due to radiogenic growth in a metasomatized lithospheric mantle. Notably, Sr-Nd-Pb isotope signatures of some Paraguayan xenoliths are similar to the isotopic composition of old sub-continental lithospheric mantle of the Brazilian Shield.

The isotopic Sr-Nd-Pb data and trace elements indicate that the lithospheric mantle prior to the enrichment event was dominated by a depleted component, isotopically resembling MORB source (or even more depleted?). Model ages (Nd-TDM) of clinopyroxenes and host rocks indicate tentatively main metasomatic events (fluids variously enriched in IE, REE and CO2) at the Brasiliano cycle (i.e. 900-460 Ma). A late, likely Cretaceous metasomatism and or small degree-melting likely caused the mismatch of element ratios (Rb/Sr, Sm/Nd, U/Pb) and respective isotope systematics by redistribution of material within the lithospheric mantle, during the different phases of lithospheric thinning in the area.

Mantle Xenoliths from intracratonic Eastern Paraguay (South America Platform) and Andean Domain: a comparison

Piero Comin-Chiaramonti[a,*], Friedrich Lucassen[b,c], Angelo De Min[a], Celso B. Gomes[d]

[a]*Earth Science Departement, Trieste University: Via Weiss 8. I-34127 Trieste, Italy.*

[b]*GeoForschungsZentrum Potsdam, Telegrafenberg, 14473 Potsdam, Germany.*

[c]*Technische Universität Berlin, Fachgebiet Petrologie – ACK 9 Ackerstr. 71-76; 13355 Berlin, Germany*

[d]*Celso de Barros Gomes, Instituto de Geociências, USP, Rua do Lago 562, CEP 05508-080, São Paulo-Brazil*

[*]*Corresponding author. E-mail address: comin@univ.trieste.it*

Protogranular spinel-peridotite mantle xenoliths and host sodic alkaline lavas of Cretaceous to Paleogene age from ≈ 26°S, central eastern Paraguay and Andes are studied for: (1) trace element behaviour; (2) Sr-Nd-Pb relationships among host lavas, mantle xenoliths and hosted pyroxenes. The mantle xenoliths are distinct into two main suites, i.e. LK (relatively low in K and incompatible elements, IE) and HK (high in K and IE), both ranging from lherzolite to dunite and showing trends of "melt extraction". The hosted clinopyroxenes display extremely variable enrichment/depletion behaviours, mainly LREE. The enriched components were mostly trapped in clinopyroxenes that previously crystallized from depleted to quasi-chondritic mantle sources. Oxygen isotopes (clinopyroxene-olivine pairs) suggest equilibration temperatures higher in the HK suite than in LK suite.

Sr–Nd–Pb isotope ratios of alkaline mafic intra-plate magmatism constrain the isotopic compositions of the lithospheric mantle. Most small-volume sodic lavas were derived from a depleted lithospheric mantle source with rather uniform initial $^{143}Nd/^{144}Nd$ (0.5127–0.5128) and $^{87}Sr/^{86}Sr$ (0.7032–0.7040). The initial $^{206}Pb/^{204}Pb$ ratios are variable (18.5–19.7) at uniform $^{207}Pb/^{204}Pb$ ratios (15.60±0.05). The variable Sr , Nd and Pb ratios are different from depleted mantle (DM), enriched (EM), or high-μ (HIMU) mantle reservoirs and probably due to radiogenic growth in a metasomatized lithospheric mantle. Notably, Sr–Nd–Pb isotope signatures of some Paraguayan xenoliths are similar to the isotopic composition of old sub-continental lithospheric mantle of the Brazilian Shield.

The isotopic Sr-Nd-Pb data and trace elements indicate that the lithospheric mantle prior to the enrichment event was dominated by a depleted component, isotopically resembling MORB source (or even more depleted?). Model ages (Nd-TDM) of clinopyroxenes and host rocks indicate tentatively main metasomatic events (fluids variously enriched in IE, REE and CO_2) at the Brasiliano cycle (i.e. 900-460 Ma). A late, likely Cretaceous metasomatism and or small degree-melting likely caused the mismatch of element ratios (Rb/Sr, Sm/Nd, U/Pb) and respective isotope systematics by redistribution of material within the lithospheric mantle, during the different phases of lithospheric thinning in the area.

Intra-plate magmatism; Sub-arc mantle; Andes, Eastern Paraguay, mantle xenoliths, clinopyroxenes, mantle metasomatism.

Introduction

Eastern Paraguay, central South America, extends in an intercratonic region including the westernmost side of the Paraná-Angola-Edendeka system (PAE) and it is located between the compressional Andean and extensional Atlantic systems (Fig. 1; cf. Gudmundsson & Samdridge, 1998 At the Paraguay latitude, the exact limit between Andean and Atlantic systems is unknown due to the presence of the Chaco-Pantanal Paleogene-Neogene basin. The seismic-tomography images show two high velocity features beneath Paraguay (P-waves; cf Fig. 1B), up to about 200 km and more than 450 km depth, respectively, the latter probably being part of the subducting Nazca slab (Liu et al., 2003). A low-velocity anomaly (Fig. 1B) in the upper mantle and mantle transition zone (MTZ) was interpreted as a fossil plume by VanDecar et al. (1995). However, the thinning of the MTZ has not been observed and Liu et al. (2003) suggest that either this thermal anomaly does not extend into the MTZ, or, alternatively that the observed anomaly is not primarily thermal, and rather dominantly compositional in origin (e.g. "veined" mantle).

Mantle derived magmatism and mantle xenoliths of Cretaceous to Early Cenozoic age are the primary sources of information on the thermal and compositional state of the uppermost mantle. This contribution reviews the existing information with a focus on the evidence from mantle xenoliths associated with the magmatism.

Late Mesozoic to Early Cenozoic intra-plate magmatism

Eastern Paraguay is characterized by: a) potassic alkaline-carbonatitic magmatism (ca. 140-126 Ma, Comin-Chiaramonti et al., 2007); Serra Geral flood tholeiites (133±1.1 Ma; Renne *et al*., 1992), both represented by high-Ti and low-Ti variants (cf. Bellieni et al., 1986); c) late Early Cretaceous to Paleogene sodic alkaline complexes, plugs and dykes (Velázquez et al., 2006).

Fig. 1

The most recent magmatism, is exclusive to southeast and central Paraguay, respectively (cf. Fig. 1), being concentrated at the Misiones and Asunción provinces, and characterized mainly by mafic-ultramafic sodic magmatism (Comin-Chiaramonti et al., 1986, 2001, 2007; Velázquez et al., 2002; 2006).

Pre-Cenozoic, mainly Cretaceous rift systems, developed at the Pacific side of the continent mainly on crust intensely worked in Early Paleozoic, which delimitates the western part of the Brazilian shield (Fig. 1; cf. Lucassen et al., 2002; 2007). Notably, small volumes of rock-types similar to those from Paraguay are widespread along the Central Andes (19-28°S) related to extensional structures (Lucassen et al., 2007) in the hinterland of an active continental margin (Fig. 1). The age of the magmatism spans from 119 Ma (Misiones; Velázquez et al., 2006) to 59 Ma (Asunción; Comin-Chiaramonti et al., 2007) and from about 130 Ma to 80 Ma (Central Andes; Lucassen et al., 2002, 2007). Both Paraguayan and Andean occurrences are characterized by the presence of mantle xenoliths in spinel facies, which vary in size from a few centimetres to 45 cm (Comin-Chiaramonti et al:, 2001; Lucassen et al., 2005). Notably, assuming a diameter of 45 cm, corresponding to the size of the largest xenoliths, a density of 3.3 g/cm^3 and an origin of the host liquids from depth ~70-75 km (~boundary between garnet and spinel peridotite), the transport of the xenoliths to the surface occurred in a very short time (e.g. less than 9 days: s. Spera, 1984; cf. Comin-Chiaramonti et al., 1991).

Table 1.

Ultramafic xenoliths, occasionally hosted by alkaline lavas and generally associated with the magmatism in continental rift areas, provide the opportunity for a direct sampling of the subcontinental mantle. Several studies on mantle xenoliths have pointed out that incompatible

trace elements, radiogenic isotopes and the major element chemistry are largely decoupled from the coherent variation that would be expected by simple extraction during partial melting of a peridotite at mantle conditions (cf. Frey and Prinz, 1978). In particular, variable enrichment of incompatible elements is commonly observed in contradiction to the refractory nature of the xenoliths, thus requiring additional processes besides partial melting and fractionation. Such processes have been generally called *metasomatic* (e.g. Menzies and Hawkesworth, 1987). Following the latter authors, metasomatism of residual peridotites by volatile-charged fluids or small-volume melts carrying incompatible elements cause different styles of enrichments. Metasomatically changed parent/daughter element ratios could develop isotopic inhomogeneities by radioactive insitu decay in a non-convective, lithospheric mantle.Geochemical and isotopic data of mantle xenoliths provide valuable information about the nature and timing of differentiation and possible metasomatism of mantle domains.

Characteristics of the host lavas

The Asunción and Misiones lavas ($^{40}Ar/^{39}Ar$ ages 58.4±2.1 and 118.3±0.9, respectively; Comin-Chiaramonti, et al., 2007) are melanephelinites and subordinate ankaratrites, according to the nomenclature after De La Roche (1980, 1986; cf. Fig. 2) and Le Maitre (1989), with mg# [MgO/(MgO+FeO), assuming Fe_2O_3/FeO ratio = 0.21] ranging from 0.64 to 0.67 (Comin-Chiaramonti et al., 1991). Representative and average analyses are reported in Table 1.

The Andean lavas and dykes are ankaratrites (Finca del Rodeo, mg# 0.67), basanites (Las Conchas + Cadillal and Betanzos, mg# 0.70 and 0.59, respectively) and tephrites (Belén, mg # 0.57). K-Ar data (Lucassen et al., 2007) give 82±4 Ma (Betanzos), 96±4 Ma (Finca del Rodeo), and about 100 to 130 Ma (Las Conchas + Cadillal and Belén, respectively).

All these rock-types belong to the sodic alkaline suites (inset of Fig. 2), having Na_2O/K_2O ratio ranging from 2.12 to 5.85. Their phenocryst population is characterized by olivine (1-7 vol%,

Fo 89-85; 1-6 vol% microphenocrysts, Fo 82-77 mole%), clinopyroxene (1-6 vol%; mg# ~0.8), Ti-magnetite (0.3-0.7 vol%; 37.9 ulv. mole%), and occasional phlogopite, e.g., in the Betanzos rocks. The hypocrystalline groundmass is made up by clinopyroxene (39-46% vol%, mg# ~0.75); olivine (3-6 vol%, Fo 74-76 mole%); magnetite (4-7 vol%, 42.8% ulv.mole%); nepheline (16-21 vol%); and glass (11-25 vol%).

Fig. 2.

Trace element and REE patterns display a similar topology (Fig. 3). The major difference is the variable Rb contents, which is higher in the Paraguayan rocks than in their Andean analogues (K/Rb: 130.2 to 205.4 in Paraguay vs. 342-1142 in the Andes). The overlapping compositions of Paraguayan and Andean magmatism are apparent, except for the Las Conchas+Cadillal basanites (mg# 0.70) that are Rb and LREE depleted with respect to the other rocks. K is systematically strongly depleted with respect to neighbouring elements, whereas (Ta)-Nb and Sr tend to show positive spikes. (Eu/Eu*) is negative in Paraguay, ranging from 0.75-0.85 and near the unity in the Andean domain (1.01-1.03; cf. Tab. 1 and Fig. 3B).

Melting models indicate that these rocks derived from liquids representing 4-6% degrees of a garnet-peridotite (cf. Comin-Chiaramonti et al., 1997) and that these liquids cannot be derived from sources similar to those represented by the enclosed spinel-peridotite xenoliths.

Radiogenic isotopes

Averaged Sr-Nd-Pb isotopic compositions (time integrated) representative of the Cretaceous to Paleogene magmatic rocks are reported in Table 2.

Due to the high Sr and Nd contents of the mafic alkaline rocks compared to crustal values of these elements, it is reasonable to assume that Sr-Nd isotopic compositions have not been

significantly affected by crustal contamination processes (see below). Therefore, Sr_i and Nd_i isotopic compositions are considered to represent the isotopic composition of their mantle source (cf. Comin-Chiaramonti et al., 1997; Lucassen et al., 2007).

The Sr-Nd isotopic variations (Fig. 3C-D) could be explained: a) by distinct portions of a large- and small-scale heterogeneous lithospheric mantle source, where the small-scale heterogeneity is required to explain the variations in the Sr_i and Nd_i ratios of each magmatic event; or b) in terms of mixing by involving an enriched mantle component with (EMI or K-ASU end–member for subcontinental lithospheric mantle?; cf: Comin-Chiaramonti et al., 1997; Antonini et al:, 2005) and depleted mantle component(s) like DMM and/or HIMU. Depleted mantle sources appear to be important in the Argentina Central Rift (Lucassen *et al*., 2002) and also in the Ayopaya alkaline-carbonatitic province, Bolivian Central Andes, which represents the petrologically most exotic expression of large-scale Mesozoic continental rifting along the western South American continent (Schultz *et al*., 2004). In any case (Fig. 3C-D), it is inferred that depleted mantle domain(s) played progressively a major role in the genesis of alkaline magmatism in Eastern Paraguay and Argentina since Cretaceous up to Paleogene times (Comin-Chiaramonti et al., 1999; Lucassen et al., 2002, 2007).

Fig. 3.

Pb isotopes are believed to discriminate between EM, DMM, and HIMU components (cf. "Mantle components" reviews e.g. Zindler and Hart, 1986; Hofmann 1997). The initial Pb isotopic compositions of the Paraguayan K-magmatism, most "primary" rock-types (cf. Antonini *et al*., 2005), have initial $^{206}Pb/^{204}Pb$, $^{207}Pb/^{204}Pb$ and $^{208}Pb/^{204}Pb$=16.888-17.702, 15.433-15.620 and 37.156-37.915, respectively. The initial lead isotopic ratios of the tholeiitic Paraguayan rocks generally agree with the Brazilian analogues reported by Marques et al.

(1999). On the other hand, the sodic alkaline rocks have different Pb isotopic compositions and differ from the potassic analogues, having initial compositions $^{206}Pb/^{204}Pb$=18.31-19.39, $^{207}Pb/^{204}Pb$=15.56-15,67 and $^{208}Pb/^{204}Pb$=37.97-39.16.

The role of possible distinct mantle components in the genesis of the Cretaceous to Paleogene magmatism are summarized in Fig. 3C-E. In general, the potassic rocks follow the same trend as the Early Cretaceous tholeiites and the Cretaceous and Paleogene sodic rocks. It is interesting to observe that the isotopic compositions trend towards the HIMU field rather than to the DMM one, particularly in the $^{207}Pb/^{204}Pb$ vs. $^{87}Sr/^{86}Sr$ and $^{143}Nd/^{144}Nd$ diagrams, suggesting that a HIMU component played an important role in the whole Cretaceous to Paleogene magmatism. However, the Pb isotopic compositions of some alkaline rocks (e.g. potassic rocks with highest $^{207}Pb/^{204}Pb$) tend towards the field of the basement rocks and, therefore, some contribution of crustal components can not be ruled out.

Alternatively, the observed trends can be modelled by mixing process between the K-ASU magmas (as defined by Comin-Chiaramonti et al., 1997) with the lowest initial $^{206}Pb/^{204}Pb$ ratios and St. Helena HIMU magma-types.The calculated patterns show that a) 10-30% of the St. Helena (HIMU end-member) is consistent with the isotopic heterogeneity observed in the potassic magmatism; b) the HIMU component appears to be dominant in the generation of the sodic magmatism.

Table 2.

Mantle xenoliths

The mantle xenoliths are mainly spinel-lherzolites, harzburgites and subordinate dunites and correspond to the Cr-diopside series of Wilshire and Shervais (1975). The dominant texture is protogranular, rarely tabular or porphyroclastic (Demarchi et al., 1988; Lucassen et al., 2005).

The Paraguay mantle xenoliths contain variable amounts of glassy patches ("blebs"), and glassy drops in clinopyroxenes. The latters show an overprinted spongy texture, characteristic of the clinopyroxenes of H-K suite (see below). The blebs (mg# 0.88-0.91) mainly consist of a glassy matrix containing microlites of olivine (mg# 0.91-0.92), clinopyroxene (mg# 0.91-0.93), Cr-spinel and (rarely) phlogopite (mg# 0.86-0.92). They are considered to have been formed by decompression melting of amphibole (cf. Wang et al., 2007) and phlogopite (Comin-Chiaramonti et al., 1986; 2001). In the Andes, clinopyroxene in some samples shows rims of secondary pyroxene with sieve texture and pockets of devitrified glass (Lucassen et al., 2005). , Blebs and secondary pyroxene rims are likely caused by decompression melting during the rapid ascent. The rapid ascent is also testified (in addition to petrophysical evidences and the persistence of glassy drops and patches mentioned above) by the lack of any apparent interactions between the mantle xenoliths and host lavas (Demarchi et al., 1988) and by lack of phase transitions in the associated crustal xenoliths (e.g. plagioclase-microcline, quartz-sillimanite pairs etc for which the calculated T-P equilibria are 570-700°C and 4-8.5 kbar, respectively; cf. Orué et al., 1990).

The Paraguay xenoliths are characterized by a large range of K_2O contents (0.02 to 0.51 wt %). Some xenoliths have K_2O abundances comparable or even higher than those reported for metasomatized mantle peridotites (e.g. Frey and Prinz, 1978; Roden et al., 1984), resembling in some case amphibole-mica-apatite bearing mantle-xenolith suites (cf. 'O Reilly and Griffin, 1988). K_2O contents and the occurrence of blebs and glassy drops allow to group the Paraguay xenoliths into two main suites, i.e. a low-K suite (LK, $K_2O < 0.1$ wt %), and a high-K suite with abundant glassy drops and/or variable amounts of blebs (HK, $K_2O \geq 0.2$ wt %). On the other hand, the Andean xenoliths have K_2O content < 0.08 wt% (average 0.02± =0.02 wt%) Complete sets of chemical analyses are in Demarchi et al (1988) and Lucassen et al. (2005).

Coherent variations of major element contents in both suites follow a dunite-lherzolite sequence trending to primitive mantle compositions (Fig. 4A). The population is mainly represented by

harzburgitic compositions, being mostly within 0.55-0.63 range of $(SiO_2+Al_2O_3)/(MgO+FeO_t)$ molar ratio. The residual character of the mantle xenoliths, believed to be consistent with melting and basalt-component removal, is shown also by the decrease in the cpx/opx modal ratio with decreasing modal cpx, which fits the model variation trend induced by partial melting of lherzolite (Fig. 4B).

Fig. 4.

Mineral Phases

Clinopyroxene (Cpx, mg# 0.90-0.96; 1 to 26 vol%) exhibits a variable morphology and composition in the Paraguayan samples, ranging from well preserved (lherzolite) to relics-spongy (dunite) crystals. The most common Cpx habitus, occurring in the cores and margins of the xenoliths of the HK suite, is represented by crystals with partially to completely "spongy" texture, due to glassy drops. Usually Cpx shows lamellar spinel (rarely orthopyroxene) exsolutions cut by the glassy drops. Because of the spinel exsolutions and glassy drops, Cpx has been analized (microprobe analyses) both on spots and "traverse" (the latter obtained by shifting the sample under defocussed beam in order to provide an extimate of composition before unmixing). The "traverse" compositions of spongy Cpx from highest K_2O -bearing xenoliths are anomalously rich in K_2O (up to 1.22 wt %). This reflect the occurrence of the glassy drops (up ~ 7.5% of the whole cpx composition, as from mass balance) whose compositions are variable, but are systematically rich in K_2O, Al_2O_3, Rb, Sr, and Ba (cf Demarchi et al. 1988). Clinopyroxenes in the Andean samples are of rather restricted composition and comprise (aluminian, sodic, ±chromian) augite to diopside with quadrilateral components > 87% (Lucassen et al., 2005)

Orthopyroxene (Opx, mg# 0.90-0.93; 3 to 30 vol%) is unzoned and rarely shows spinel exsolutions.

Olivine (Ol, 60 to 97 vol%) is chemically homogeneous within each samples and varies in composition mainly from Fo 89 (lherzolites) to Fo 93 (dunites) mole%.

Spinel (Sp, 0.6 to 4 vol%) from xenoliths with $K_2O \geq 0.20$ wt % (see below) is generally characterized by Cr increase from the core to the rim, particularly grains inside the blebs, while spinels from xenoliths with $K_2O < 0.1$ wt % are unzoned (Demarchi et al.1988). The Cr/(Cr+Al) atomic ratio shows a main variation range between 0.10 and 0.70.

Sulfides (pyrrhotite and pentlandite) and *apatite* occur in very small amounts as dispersed grains in almost all the xenoliths.

Carbonate

In Paraguay carbonates are present in pockets in the glassy patches, or as carbonate veins along the grain boundaries. They are Mg-rich calcite ($MgCO_3$ about 5-10 wt% and < 0.6 wt%). Measured $\delta^{18}O$‰ (SMOW) and $\delta^{13}C$‰ (PDB) in two representative samples (HK suite) give +8.5±0.5 and -7.4±0.9, respectively, i.e. values within the field believed typical of primary carbonatites, according to Keller and Hoefs (1995).

In the Andes occurrences, Lucassen et al. (2007) report the presence of carbonatized peridotites, similar in shape and size to the other peridotite xenoliths. Minor clinopyroxene and spinel and occasional phogopite are set in a matrix of carbonate grains. $\delta^{18}O$‰ and $\delta^{13}C$‰ range from +17.3 to +20.7 and from -5.3 to -8.9, respectively, and indicate post magmatic and/or deuteric-groundwater processes in the carbonate formation (cf. Comin-Chiaramonti et al., 2005).

The "residual" character of the xenolith suites indicated by their major element compositions is also reflected by the compositional variations of mineral phases (Demarchi et al., 1988; Petrini et al., 1994), i.e. Mg/Fe_{tot} (atomic ratio) of the orthopyroxene (9.7 to 11.8) is correlated with the Fo content of the olivine (90 to 93) and with Mg/Fe_{tot} of clinopyroxene (9.2 to 15.3), as well as with the Cr/(Cr+Al) ratio of the spinel (0.10 to 0.70).

Thermobarometry

In Paraguay, intercrystalline equilibration temperatures for orthopyroxene-clinopyroxene pairs (Wells geothermometer, 1977) and for olivine-spinel pairs (Fabriès geothermometer, 1979) vary between 862 and 1075 °C and between 748 and 968°C, respectively. Intracrystalline pressures (calculated according to Mercier, 1980) vary between 11-23 Kb and 17-20 Kb for clinopyroxene and orthopyroxene, respectively (cf. Petrini et al., 1994) in both the two suites, where the higher pressures where obtained for the more depleted xenoliths of the LK-suite (cf. Prncivalle et al., 2000; Comin-Chiaramonti et al:, 2001).

The oxygen isotope compositions on separates of clinopyroxene and coexisting olivine ($\delta^{18}O$‰) range from 5.5 to 6.0‰, and from 5.0 to 6.1‰, respectively (Table 1 of Comin-Chiaramonti et al., 2001). These measured isotopic ratios are in the range of values for worldwide mantle phases (olivine 4.4 to 7.5‰, clinopyroxene 4.8 to 6.7‰; cf Chazot et al., 1994 and therein references) and for South America mantle xenoliths (olivine 4.9 to 6.4‰, clinopyroxene 5.0 to 6.0‰; cf Kyser, 1990). The calculated Cpx-Ol isotopic temperatures (calculated according Kyser et al., 1981) are around 970-1070°C (LK suite) and 1100-1180°C (HK suite), respectively, whereas the Mercier's intracrystalline temperatures are 970-1010°C (LK) and 1005-1050°C (HK), respectively (cf. Petrini et al., 1994; Princivalle et al., 2000).

Notably, the $\delta^{18}O_{cpx}$ vs $\delta^{18}O_{ol}$ diagram (Fig. 5A) shows different trends for LK and HK suites, reflecting differences that vary with apparent isotopic equilibration temperatures. In particular the O-isotope temperatures vary coherentely with the $\Delta^{18}O$(cpx-ol) which tends to 0 in the HK (Fig. 5B). The Mercier's temperatures vs $\Delta^{18}O$(cpx-ol) show that HK samples have equilibration temperatures higher than the LK analogues (Fig. 5B). To be noted that the LK samples plot below, but near to the experimentally determined fractionation line (Chiba et al., 1989), whereas the HK-types have less significant O-isotopic fractionation between minerals compared to LK samples (Fig. 5C).

According to Princivalle et al. (2000), the investigated Paraguay clinopyroxenes have V(Cell) and V(M1) sites intermediate between those of plagioclase- and garnet-bearing mantle peridotites, i. e, in a pressure range between 12 and 22 kbar (cf. also Nimis and Ulmer, 1998). The ranges of temperature and pressure calculated for the mantle xenoliths from intracratonic Paraguay overlap with those of the mantle xenoliths from the Central Andes, which indicate T 900-1190°C and P13-18 kbar (calculated maximum pressures for garnet-free mineral assemblage; Lucassen et al., 2005).

Fig. 5. **A**

Clinopyroxenes

The mantle clinopyroxenes play an important role for the interpretation of mantle processes, such as melting and metasomatism (e.g. Salters and Shimizu, 1988; Takazawa et al., 1992; Vannucci et al., 1994; Laurora et al.,2001. Wang et al., 2007). The decrease of modal clinopyroxene and depletion indexes of whole rock and clinopyroxene (cf Fig. 4), from fertile peridotite (primitive mantle) towards harzburgite-dunite are consistent with the extraction of melt. Melt extraction has a substantial impact on the concentrations of trace elements of the clinopyroxene in general and the incompatible trace elements in particular (cf. Rivalenti et al., 1996). Clinopyroxene is the principal host of important trace elements as Sr, U, Th, Pb and REE in garnet and amphibole free paragenesis (cf. Gregoire et al:., 2000).

In this section, we examine trace element and Sr and Nd isotopic compositions of the clinopyroxenes from selected Paraguay and Andes mantle xenoliths, LK and HK suites, respectively.

Tab. 3.

Fig. 6.

Fig. 7.

Trace Elements

Trace element analyses are given in Table 3. The main characteristics are summarized in the extended trace element and REE diagrams of Figs. 6 and 7. The clinopyroxenes from both, LK and HK suites show variable enrichment of La, Ce, Sr, and Nd, from flat to fairly steep distribution patterns independently of the Cpx content, (i.e. melting degree of the xenoliths) and of the calculated temperatures. The orthopyroxene exsolutions (e.g. LK-3254 specimen) and their host clinopyroxene have similar distribution patterns for the more compatible elements, but K, LREE and Sr are strongly depleted in opx (Fig. 6C). In particular, the HK-3284 clinopyroxene (Cpx = 1%, with glassy drops up to 7.5%; panels E of Fig. 6 and 7) appears strongly enriched in REE, comparable to the hosted glassy drops.

LREE are commonly strongly enriched (Paraguay: La_N/Yb_N, LK suite, lherzolite = 11.9-5.4, harzburgite ~ 55; HK suite: lherzolite = 20.3 - 16.2, harzburgite = 98.2 - 7.9), excluding samples 3227 (LK harzburgite with La_N/Yb_N = 0.92) and 3222 (HK lherzolite with La_N/Yb_N = 17.66 to =0.65; LK Andes La_N/Yb_N = 110-0.5; cf. Comin-Chiaramonti et al., 2001, Lucassen et al., 2005, and Table 3). The contents of incompatible trace elements is not consistent with the fractional melting processes indicated by the major element composition. Only few samples have trace element contents consistent with melt extraction (e.g., HK lherzolite 3222 of Comin-Chiaramonti et al:, 2001; panel G of Fig. 6 can be modelled by low degree (6%) of non-modal fractional melting of primitive mantle; see also also Rivalenti et al., 2000).

In the normalized trace element diagrams (Fig. 6), all the samples have patterns depleted in Ba, Nb, Zr and Ti. Furthermore, Zr and Ti display systematically negative spikes (cf. Rampone et al., 1991), indicating HFSE depletion (cf also Zr/Zr* and Ti/Ti* of Table 3). Sr shows both positive and negative anomalies in LK and HK suites (Sr /Sr* = 2.34 to 0.51), with the

minimum in HK harzburgite 3284 (Sr/Sr* = 0.51). In particular, Sr from the Andean clinopyroxenes (LK suite) display a positive correlation with $(La/Yb)_N$, i.e. $Sr=10.76*(La/Yb)_N+33,48$ with r=0.94 (cf. Lucassen et al., 2005). Y/Y* ratio generally is near the unity (av. 0.94 ± 0.26), but it shows a positive anomaly in the Cpx from LK harzburgite 3269 (3.09 to 1.71, core and rim, respectively) and a negative anomaly in Cpx from LK lherzolite 3221 (0.22). In particular, the xenolith A-104 (LK, Andes; Table 3) has a modal composition cpx 17.7, opx 27.3, ol 53.0, sp 2.0%, very similar to that of the primitive mantle (Hofmann,1988; cpx 18, opx 25, ol 55, sp 2%) and the I.E. and REE contents of the clinopyroxene display trends overlapping with those of the PMCE (clinopyroxene trace element compositions; cf. Rivalenti et al., 1996 and panels D of Figs 6 and 7). Moreover, cpx in the residue from non-modal fractional melting (6%) of the primitive mantle mimics the behaviour (minimum contents) of the cpx from HK suite (10-12% cpx; panel G of Fig. 6). It is worth noting that some harzburgites display U-shaped patterns (e.g. LK 3269 and HK 3211; e.g. panel C of Fig. 7), with La_N/Sm_N ~ 60 and Gd_N/Yb_N ~ 0.55 (cf Table 3 and Table 2 of Comin-Chiaramonti et al., 2001). Such characteristics were attributed to a "carbonatitic component" by Hauri (1997).

Compared with the host Cpx, the glassy drops (e.g. HK 3284 Cpx) are strongly enriched in Rb, Ba, and K, and display positive spikes for Sr (Sr/Sr*=1.679) and Zr (Zr/Zr*=1.13; cf. panel E of Fig. 6, and Table 3). Notably, the geochemical features of the glassy drops fit those of a melt from a phlogopite rich source (e.g, McKenzie and O'Nions, 1991: Ti = 4796 ppm and K= 78786 ppm). The glassy patches differ from the glassy drops by their Zr/Zr* (0.47 vs 1.13), Ti/Ti* (0.16 vs 0.69), Eu/Eu* (1.14 vs 0.83), and by a positive Nb spike (panel F of Fig. 6). The general element distribution pattern of the glassy patches is similar to that of glasses , which were interpreted by Laurora et al. (2001) as the disequilibrium melting of metasomatic assemblages (dominantly amphibole) that produced carbonated silicate melts. Correlations between $\delta^{18}O$ and IE contents were not observed (cf. Comin-Chiaramonti et al., 2001): the lack

of significant differences in oxygen isotopic composition between LREE-depleted and REE-enriched samples of both LK and HK suites suggests that metasomatism does not affected the oxygen isotope systematics.

Clinopyroxenes from Andean pyroxenite are characterized by element contents of about 1-2 times primitive mantle (Fig. 6, panel H), but with a prominent negative spike for Sr (Sr/Sr* 0.42-0.45) and Y (Y/Y* 0.67-0.78), and a slight upward-concave REE pattern (Fig. 7, panel H and Table 3). Clinopyroxene from carbonatized xenoliths display a large range of the normalized element contents between 0.1 to 10 times primitive mantle (Fig. 6, panel H) and variable REE patterns (Fig. 7, panel H).

In summary, the trace elements patterns of clinopyroxenes from Paraguyan and Andean xenoliths could be the result of different, superimposed processes affecting the upper mantle (cf: Comin-Chiaramonti et al., 2001):

depletion by variable degrees of partial melting, as shown by the "residual" character of mantle xenoliths;

subsolidus re-equilibration, as indicated by spinel and orthopyroxene exsolution in clinopyroxenes, and subsequent variations of the V(cell) and V(M1) volumes (Pricivalle et al., 2000);

metasomatic processes, as shown by variable enrichment of incompatible elements, both in the clinopyroxenes and in the host xenoliths;

decompression and partial melting after the sampling by host lavas, as shown by the presence of glassy phases, i.e. glassy drops in clinopyroxenes "cutting" the spinel exsolutions, and by the blebs in the host xenoliths.

Tab. 4.

Sr-Nd Isotopes

Rb-Sr and Sm-Nd isotope data have been determined on whole rock and on clinopyroxene-orthopyroxene separates (Table 4). Whole rocks and mineral separates fom Paraguay display a very wide isotopic variation (measured ratios), with $^{87}Sr/^{86}Sr$ ratios overlapping in the LH and HK suites and in the ranges 0.70360 - 0.70480 (WR) and 0.70326 - 0.70461 (Cpx), respectively, and $^{143}Nd/^{144}Nd$ in the ranges 0.51246 - 0.51346 (WR) and 0.51260 - 0.51348 (Cpx), respectively. In the Andean Cpx are mainly in the ranges 0.70271-0.70478 ($^{87}Sr/^{86}Sr$) and 0.51280-0.51387 ($^{143}Nd/^{144}Nd$) and compositions from both distant areas overlap.

In Paraguay, positive correlation ($r^2 > 0.8$) between $^{87}Rb/^{86}Sr$ and $^{87}Sr/^{86}Sr$ is shown by xenoliths (whole-rocks) of the two suites, from which a reference lines of 128 Ma can be calculated for the two suites (cf. inset Fig. 6B of Comin-Chiaramonti et al., 2001). $^{87}Sr/^{86}Sr$ and $^{87}Rb/^{86}Sr$ ratios of the pyroxenes are poorly correlated with the 128 Ma reference line, reflecting substantial isotopic disequilibria between whole rock and hosted clinopyroxene (cf. Song and Frey, 1989). The $^{87}Sr/^{86}Sr$ xenolith whole rock - clinopyroxene disequilibria could be ascribed to contributions of a component enriched in radiogenic Sr to the bulk xenoliths (cf. Downes and Dupuy, 1987). This component actually may be confined to the blebs, to glassy drops, and/or glass at grain boundaries. The leaching of the whole rock samples possibly was not enough strong to dissolve such an enriched phase, as in the case of glassy component of the clinopyroxene. The leaching solutions produce errorchrone lines (Table 4 of Comin-Chiaramonti et al., 2001) between 129 Ma (LK sample 3192) and 61 Ma (HK sample 3307), approaching the ages of the K-alkaline magmatism (128 Ma) and nephelinitic magmatism of the region (60 Ma), respectively (Velázquez et al., 2006). Probably, an isotopic mixing between an old whole-rock component (?) and the magmatic-decompressional event (Early Cretaceous to Paleogene) affected the clinopyroxenes and the host xenoliths.

The Early Cretaceous age approaches those inferred for potassic and tholeiitic rocks (128 and 133 Ma, respectively; Comin-Chiaramonti and Gomes, 1996, 2005; Ernesto et al., 1996) from Asunción-Sapucai-Villarrica graben. Notably, the Early Cretaceous age may indicate the latest thermal event affecting the lithospheric mantle before the sampling by ascending melanephelinite magma in the late Early Cretaceus to Eocene times in Eastern Paraguay. In the Andes the age of equilibration of the lower crust xenoliths and the eruption of the host lavas is around 100 Ma (Lucassen et al., 2005). Thus measured isotope ratios of the analyzed samples (Table 4) were corrected for in situ decay to ages of 128 and 100 Ma for Paraguay and Andes, respectively.

The initial $^{87}Sr/^{86}Sr$ and $^{143}Nd/^{144}Nd$ ratios of whole rocks and clinopyroxenes (Fig. 8) encompass the whole range of isotopic ratios observed in NE Brazil (Pico Cabuji), Fernando de Noronha island and Patagonia xenoliths (cpx compositions; Rivalenti et al., 2000; Barbieri et al., 1997; Stern et al., 1989). The xenoliths compositions partly overlap with the ratios of their host rocks (Fig. 8). $^{87}Rb/^{86}Sr$ ratios of the clinopyroxenes are systematically lower than those of their host rocks, and cluster between 0.0002 and 0.0086; only one sample from LK suite and two samples from HK suite have $^{87}Rb/^{86}Sr$ ratios above 0.1 (cf Table 3 of Comin-Chiaramonti et al., 2001 and Table 3 of Lucassen et al:, 2005).

The initial $^{143}Nd/^{144}Nd$ ratios span from enriched (0.51237) to depleted (0.51372) signatures (Table 4; Fig.8). The Nd isotope ratios of the Paraguay - Andes xenoliths and hosted pyroxenes encompass almost the entire range of values reported for mid ocean ridge basalts (MORB) and ocean island basalts (OIB) (cf White, 1985; Galer and O'Nions 1989; Stosch and Lugmair, 1986). Significant correlations between $^{147}Sm/^{144}Nd$ and $^{143}Nd/^{144}Nd$ were not observed ($r^2 \leq 0.85$), but the best fitting is along a 0.5 Ga line (cf. Table 4 of Comin-Chiaramonti et al., 2001). On the contrary, strongly positive correlations are shown by the clinopyroxenes from Pico Cabuji (NE Brazil; $r^2 = 0.99$, best fitting at 1110 Ma) and from Fernando de Noronha ($r^2 = 0.90$,

best fitting at 413 Ma; cf Table 4 and Fig. 6B of Comin-Chiaramonti et al., 2001). At any way, to be noted that the Paraguay xenoliths tend to fit the "Paraguay array" of Comin-Chiaramonti et al., (1997). In many of the Andean $^{147}Sm/^{144}Nd$ (too low or 'enriched') do not fit the observed $^{143}Nd/^{144}Nd$ (too radiogenic) ratios and young enrichment is needed in the Andean case to explain these relationships. The poor fit of $^{143}Nd/^{144}Nd$ and $^{147}Sm/^{144}Nd$ for clinopyroxenes could have variable causes, initial Nd isotope heterogeneity, variable ages or intensity of the metasomatic overprint or depletion by melt extraction.

Fig. 8

In particular, the $^{143}Nd/^{144}Nd$ ratios of clinopyroxenes and orthopyroxene indicate isotopically heterogeneous mantle sources, ranging from values approaching the Bulk Earth estimate (e.g. HK-3288-Cpx: measured $^{143}Nd/^{144}Nd$ = 0.51267) to a variably LREE depleted source (e.g. LK-3254-Cpx: $^{143}Nd/^{144}Nd$ = 0.51348). Sample 3252 (LK) shows significant whole rock-clinopyroxene-orthopyroxene isotopic disequilibria, i.e. measured $^{143}Nd/^{144}Nd$ = 0.51311, respectively, and $^{147}Sm/^{144}Nd$ = 0.16, 0.11 and 0.10, respectively (cf: Table 4). Thus, the decoupling between $^{143}Nd/^{144}Nd$ and $^{147}Sm/^{144}Nd$ ratios suggests a complex history of REE depletion and enrichment events in the mantle, as envisaged by the trace element patterns.

The higher $^{87}Sr/^{86}Sr$ ratios for whole rocks, and acid leachates relative to clinopyroxenes indicate that the Sr isotopic ratio was affected by secondary processes. Therefore, model age (depleted mantle) calculations based on Rb/Sr systematics are not reliable. Sm/Nd model ages (TDM), calculated with respect to a depleted reservoir (Table 4), range from 109 to 921 Ma (average LK Paraguay = 0.46 ± 0.26 Ga, HK, 0.50 ± 0.12 Ga, and LK-Andes 0.49 ± 0.09 Ga), except the pyroxenite for which a model age of ~1410 Ma was calculated. Unfortunately, Nd model ages are highly problematic in metasomatically overprinted rocks, which are seen in the mismatch of $^{147}Sm/^{144}Nd$ and $^{143}Nd/^{144}Nd$ ratios. The approach relies on a refractory Sm/Nd

system after separation of the respective batches from the depleted mantle or requires a good control (time and composition) of changes in the Sm/Nd system in the respective batch.

The Sm/Nd model ages (TDM), calculated with respect to a depleted reservoir (Table 4), range from 110 to 920 Ma (average LK = 0.46 ± 0.26, HK, 0.50 ± 0.12 Ga, respectively, where LK-Andes show 0.49 ± 0.09 Ga, clustering the Brasiliano cycle, i.e. 900-460 Ma, according to Hartmann et al., 2000), pyroxenite excepted for which a model age of 1413 Ma was calculated. The complexities of the Sm/Nd systematic suggests a multi-stage history, such as melt extraction and fluid or melt addition, which all could be highly variable and occur repeatedly and were preserved in the lithospheric mantle beneath Paraguay and Andes at different times.

Lead Isotopes

Lead isotopes are available for the clinopyroxenes from Andes (Lucassen et al., 2005) and for two whole rock samples from Paraguay (Table 5). Xenoliths from both distant areas, Paraguay and the Central Andes, show similar Pb isotope compositions (Fig. 9). The $^{206}Pb/^{204}Pb$, $^{207}Pb/^{204}Pb$, $^{208}Pb/^{204}Pb$ ratios vary between 17.7 and 20.6, 15.5 and 15,7, 38.1 and 41.9, respectively, but the majority of the samples cluster in the much smaller field of their host lavas and the Bolivian Ayopaya carbonatite (Schultz et al., 2004). The $^{238}U/^{204}Pb$ (μ ratio) is below the typical depleted mantle value of ca. 8 (except sample A-147-m with μ ~55). There is again as in the case of the Sm-Nd isotope system a mismatch between parent/daughter ratios and the radiogenic isotope composition (Table 5) and a metasomatic overprint or melt extraction relatively late in the history of the lithospheric mantle is required.

The isotopic compositions of many samples, roughly plot in between EMI, DMM and HIMU mantle end members (Fig. 9; cf. Zindler and Hart, 1986; Stracke et al., 2003) and could be tentatively explained by a mixing scenario (metasomatism), which adds a HIMU signature from

an external source (convective mantle) to a EM1 lithosphere (cf. Figs. 3 and 9). However, there are also a number of samples, which do not fit such a simple trend.

Table 5.

Discussion and Conclusive remarks

Paraguay and Andes spinel peridotites, which occur at similar latitudes, are variable in major element compositions, ranging from relatively "fertile" to very depleted in basaltic component. Two suite can be distinguished: low and high in K_2O content ($K_2O < 0.1$ and >0.1, LK and HK, respectively).The HK suite is restricted to xenoliths from Paraguay and some of these xenoliths have exceedingly high K_2O and incompatible elements (IE) compared to the composition of lherzolites which underwent partial melting during basalt-extraction (cf. Frey and Green, 1974). The major element of the xenoliths are largely consistent with residual compositions after variable degrees of partial melting, but metasomatic effects are apparent above all in the HK suite. The incompatible element contents of clinopyroxenes from LK and HK is highly variable similar to other world-wide occurrences (cf. e.g., Salters and Shimizu, 1988). Trace element enrichment suggests that some processes, other than depletion, played an important role in the xenoliths (cf. Fig. 6).

Paraguayan and Andean clinopyroxenes display very variable REE enrichments (Fig.7), which are not bound to a specific major element composition or mineralogy. Only in few Paraguayan samples, the enrichments appear to be more pronounced in clinopyroxene with spongy textures and glassy drops. Considering the radiogenic Nd isotope compositions and the low Sm/Nd ratios in many clinopyroxene, this enrichment occurred probably late in the history of the xenoliths and it affected xenoliths with different isotopic signatures, i.e. equally with radiogenic and relatively unradiogenic isotope signatures. The U-Pb system indicates also a late

metasomatic event, with the removal of U from the rocks (or enrichment of Pb). The radiogenic isotope signatures of the xenoliths do not fit any of the canonical mantle end-members. They span a broad compositional field, most samples with Sr and Nd isotope compositions indicating the contribution of depleted mantle, but some samples show also affinity to enriched mantle of the EMI-type typical of old subcontinental mantle known from the Brazilian Shield (cf. Fig. 8). Pb isotope compositions are also variable, but most samples are more radiogenic than average depleted mantle and indicate the influence of an HIMU source (Fig. 9). The magmatic host rocks of the xenoliths have a broadly similar isotopic composition (cf. Figs 3 and 9), but some xenoliths samples show extreme compositions.

There are two hypothetical end-member scenarios for creating heterogeneous isotope compositions in the lithospheric mantle sources: (1) radiogenic in-situ growth during long-term separation from convection and (2) metasomatism of the lithospheric mantle by infiltrating melts from an external source, i.e. the asthenosphere (depleted mantle) or deeper mantle sources (e.g. HIMU). The processes must be pervasive (the signatures are found in xenoliths from the uppermost mantle and in the host melts from below) and at large scale, because at least in the Andes a large N-S section shows similar signatures.

Preconditions of (1) are the existence of a reasonably old lithosphere, which formed in the Palaeozoic or Pre-Palaeozoic and ancient substantial reworking and metasomatism of this lithosphere. The pristine material of mantle lithosphere is assumed to be of asthenospheric (depleted mantle) origin. Substantial reworking probably took place at Early Palaeozoic for the Andean and similar or older for the Paraguayan section. Such scenario has been invoked for compositional unusual, high-μ intra-plate magmatism on the Arabian plate (Stein et al., 1997).

The second scenario includes infiltration of the pristine lithosphere by melts from an external high-μ source. This event(s) must be relatively young, due to the already highly radiogenic Pb compositions of the required high-μ agent. Further, this scenario requires large scale material

transport from the deeper mantle through the asthenosphere and hence a young convective (thermal) instability for the activation of the high-μ reservoir.

However, the second model creates problems at least with the Andean intra-plate magmatic rocks and xenoliths. Contemporaneous intense magmatism in the magmatic arc is clearly derived from a subduction modified depleted mantle, i.e. involves 'normal' asthenosphere without any contribution of a HIMU component (e.g. Lucassen et al., 2006). The assumption of a plume-like scenario for the intra-plate magmatism and metasomatism in the lithospheric mantle would require two separated, compositionally different large scale convection systems, which did not mix on a restricted space (distance Mesozoic arc - intra-plate magmatism is 500 present + 200 km Andean shortening ~ 700 km in the Cretaceous). Assuming an older 'plume' event this must have been without important magmatic activity. There are no indicators of a large scale melt infiltration/melting event involving HIMU in the magmatic record. The last thermal pulse recorded on a large N-S scale also far behind the arc was late Carboniferous-Permian. Mesozoic to Cenozoic magmatism was very minor and the Salta Rift (and other extensional structure) was considered as of minor magmatic activity.

The first, lithospheric scenario has the obvious advantage that it does not require additional far reaching geodynamical implications. In a first step in-situ growth of the variable isotope signatures is caused by variable old metasomatism (trace element signatures), in the case of the Andes linked to the Early Palaeozoic orogeny. Incompatible trace element distribution is easily changed by minor amounts of melting, and trace elements could be locally redistributed by trace element rich melts, with or without changes of the isotope composition. Therefore, the late metasomatism causing the mismatch of parent element contents and daughter isotope compositions could be largely autochthonous and caused by Na-alkaline basaltic magmas from deeper, possibly garnet-bearing lithospheric mantle (cf. Comin-Chiaramonti et al, 1997). Moreover, high LREE and Sr abundances coupled with depletion in Nb, Ti, Zr of some xenoliths from Paraguay could indicate carbonatite metasomatism (Comin-Chiaramonti et al.,

1991; Hauri et al. 1993). In Paraguay the situation is complicated by the occurrence of old subcontinental mantle of the Brazilian Shield, which could contribute to possible redistribution of isotope and trace element signatures by melts within the lithospheric mantle. Unfortunately little of such processes -except compositional heterogeneities- remained visible in high T environments, due to rapid recrystallization. The melt inclusions of some Paraguayan xenoliths are the only preserved visible heterogeneities linked to metasomatism.

In Paraguay, the isotopic data seem to indicate that the lithospheric mantle prior to the enrichment event was dominated by a depleted component, isotopically resembling MORB sources or even more depleted represented by residua from ancient events of partial melting. In the Andes, the composition of the source is also believed to be depleted mantle, but different from a MORB type source, showing slightly more radiogenic ^{87}Sr and less radiogenic ^{143}Nd than the Pacific MORB. The substantial compositional variations in some xenoliths and host lavas likely reflect small-scale sampling of the lithospheric mantle, and differential interactions between fluids and overlaying peridotites.

In summary, there is strong evidence for variable metasomatism in the xenoliths in both distant areas. The observed radiogenic isotope trend (Bulk Earth vs Depleted Mantle) is not consistent with major element refractory parameters, suggesting that a mixing with enriched components is also recorded at whole-rock scale.

We stress that the compositions of mantle xenoliths and host sodic alkaline lavas are surprisingly similar at about 26°S latitude in an extensional intra-cratonic environment (Paraguay) and an extensional to transpressional setting transitional between arc and craton (Andes orogen).

Work in Paraguay was financed by the Brazilian Agency FAPESP, Grants # 97/01210-4 and 01/10714-3, for the financial support. Work in the Andes was financed by Deutsche Forschungsgemeinschaft (DFG, German Research Foundation) within the Sonderforschungsbereich (SFB) 267, Deformation Processes in the Andes.

References

Antonini P., Gasparon M., Comin-Chiaramonti P., Gomes C.B., 2005. Post-Palaeozoic magmatism inEastern Paraguay: Sr-Nd-Pb isotope compositions. In: Comin-Chiaramonti P., Gomes C.B. , eds.,Mesozoic to Cenozoic alkaline magmatism in the Brazilian platform. Edusp/Fapesp, São Paulo, Brazil, 57-70.

Barbieri, M.A., Rivalenti, G., Cingolani, C., Mazzucchelli, M., Zanetti, A., 1997. Geochemical and isotope variability of the northern and southern Patagonia lithospheric mantle (Argentina). Proceedings of South America Symposium onf Isotope Geology, Campos do Jordão, São Paulo, Brazil, Extended Abstract, 41-43.

Bell, K., Tilton G.R. (2001) – Nd, Pb and Sr isotopic compositions of East African carbonatites: evidence for mantle mixing and plume inhomogeneity. Journal of Petrology, 42, 1927-1945.

Bellieni, G., Comin-Chiaramonti, P., Marques, L.S., Martinez L.A., Melfi, A.J., Nardy, A.J.R., Piccirillo,E.M., 1986. Continental flood basalts from the central-western regions of the Paraná plateau (Paraguay andArgentina): Petrology and petrogenetic aspects. Neues Yearbook Mineralogische Abhandlungen 154, 111-139.

Boynton, W.V., 1984. Cosmochemistry of the Rare Earth elements: meteorite studies. In: P. Henderson (ed.): Rare Earth Element geochemistry. Elsevier, Amsterdam, 63-114.

Bristow, J.F., 1984. Nephelinites of the North Lebombo and South East Zimbawe. Spec.Publ.Geol.Soc. South Africa 13, 87-104.

Chaffey, D.J., Cliff R.A., Wilson, B.M., 1989. Characterization of the St Helena magma source. In: D: Sunders and M.J. Norry (Editors). Magmatism in the Ocean basin. Geological Society, Special Paper 42, 257-276.

Chazot, G., Menzies, M.A., Lowry, D., Mattey, D.P., 1994. Fluid peridotite interaction in spinel facies mantle: oxygen isotopic composition of hydrous and anhydrous lherzolites. International Symposium on the physics and chemistry of the Upper Mantle, São Paulo, Brazil, Extended Abstract, 70-72.

Chen, C.Y., Frey, F.A., Song, Y., 1989. Evolution of the upper mantle beneath southeast Australia: geochemical evidence from peridotite xenoliths in Moun Leura basanite. Earth and Planetary Science Letters 93, 195-209.

Chiba, H., Chack, T., Clayton, R.N., Goldsmith, J., 1989. Oxygen isotope fractionations involving diopside, forsterite, magnetite, and calcite: Application to geothermometry. Geochimica et Cosmochimica Acta 53, .2985-2995.

Comin-Chiaramonti, P. and Gomes, C.B. (Editors). 1996. Alkaline Magmatism in Central-Eastern Paraguay. Relationships with coeval magmatism in Brazil. São Paulo, Brazil, Edusp/Fapesp, 464 pp.

Comin-Chiaramonti, P., Gomes, C.B. (Editors). 2005. Mesozoic to Cenozoic alkaline magmatism in the Brazilian Platform. São Paulo, Brazil, Edusp/Fapesp, 752 pp.

Comin-Chiaramonti, P., Demarchi, G., Girardi, V.A.V., Princivalle, F., Sinigoi, S., 1986. Evidence of mantle metasomatism and heterogeneity from peridotite inclusions of northeastern Brazil and Paraguay. Earth and Planetary Science Letters 77, 203-217.

Comin-Chiaramonti, P., Civetta, L., Petrini, R., Piccirillo, E.M., Bellieni, G., Censi, P., Bitschene, P., DeMarchi, G., De Min, A., Gomes, C.B., Castillo, A.M.C., Velázquez, J.C., 1991. Cenozoic nephelinitic magmatism in Eastern Paraguay: petrology, Sr-Nd isotopes and genetic relationships with associated spinel-peridotite xenoliths. European Journal of Mineralogy 3, 507-525.

Comin-Chiaramonti, P., Gomes, C.B., Petrini, R., De Min, A., Velázquez, V.F., Orué, D., 1992. A new area of alkaline rocks in Eastern Paraguay. Revista Brasileira de Geociências 22, 500-506.

Comin-Chiaramonti, P., Cundari, A., Piccirillo, E.M., Gomes, C.B., Castorina, F., Censi, P., De Min, A., Marzoli, A., Speziale, S., Velázquez, V.F., 1997. Potassic and sodic igneous rocks from Eastern Paraguay: their origin from the lithospheric mantle and genetic relationships with the associated Paraná flood tholeiites. Journal of Petrology 38, 495-528.

Comin-Chiaramonti, P., Cundari, A., DeGraff, J.M., Gomes, C.B., Piccirillo, E.M., 1999. Early Cretaceous-Cenozoic magmatism in Eastern Paraguay (western Paraná basin): geological, geophysical,and geochemical relationships. Journal of Geodynamics 28, 375-391.

Comin-Chiaramonti, P., Princivalle, F., Girardi, V.A.A., Gomes, C.B., Laurora, A., Zanetti, F., 2001. Mantle xenoliths from Ñemby, Eastern Paraguay: O-Sr-Nd isotopes, trace elements and crystal chemistry of hosted clinopyroxenes. Periodico di Mineralogia 70, 205-230.

Comin-Chiaramonti, P., Gomes, C.B., Censi, P., Speziale, S., 2005. Carbonatites from southeastern Brazil: a model for the carbon and oxygen isotopic variations. In: P. Comin-Chiaramonti and C.B. Gomes (Editors). Mesozoic to Cenozoic Alkaline Magmatism in the Brazilian Platform, São Paulo, Brazil, Edusp/Fapesp, pp. 629-656.

Comin-Chiaramonti P., Marzoli A., Gomes C.B., Milan A., Riccomini C., Velázquez V.F., Mantovani, M.M.S., Renne P., Tassinari, C.C.G., Vasconcelos, P.M., 2007. Origin of Post-Paleozoic magmatism in Eastern Paraguay. In: R. G. Foulger and D.M. Jurdy (Editors), The origin of melting anomalies. Geological Society of America, Special Paper 430, in preparation, available on line at www.mantleplumes.org/parana.html.

De La Roche, H., 1986. Classification et nomenclature des roches ignées: un essai de restauration de la convergence entre systématique quantitative, typologie de l'usage et modélisation génétique. Bulletin Societé Géologique de France 8, 337-353.

De La Roche, H., Leterrier, P., Grandclaude, P., Marchal, E., 1980. A classification of volcanic and plutonic rocks using R_1-R_2 diagram and major element analyses. Its relationships with current nomenclature. Chemical Geology 29, 183-210.

Demarchi, G., Comin-Chiaramonti, P., De Vito, P., Sinigoi, S., Castillo, A.M.C., 1988. Lherzolite-dunite xenoliths from Eastern Paraguay: petrological constraints to mantle metasomatism. In: E.M. Piccirillo and A.J. Melfi (Editors), The Mesozoic Flood Volcanism from the Paraná Basin (Brazil). Petrogenetic and geophysical aspects. Iag-Usp, São Paulo, Brazil, 207-227.

Downes, H., Dupuy, C., 1987. Textural, isotopic and REE variations in spinel peridotite xenoliths, Massif Central, France. Earth and Planetary Science Letters 82, 121-135.

Ernesto, M., Comin-Chiaramonti P., Gomes C.B., Castillo, A.M.C.C., Velázquez, V.F., 1996. Palaeomagnetic data from the Central Alkaline Province, Eastern Paraguay. In: P. Comin-Chiaramonti and C.B. Gomes (Editors), Alkaline magmatism in central-eastern Paraguay. Relationships with coeval magmatism in Brazil. São Paulo, Brazil, Edusp/Fapesp, pp. 85-102.

Faure, G. 1986. Principles of isotope geology. John Wiley & Sons, New York, 589 p.

Fabries, J., 1979. Spinel-olivine geothermometer in peridotites from ultamafic complexes. Contribution to Mineralogy and Petrology 69, 329-336.

Frey, F.A., Green, D.H., 1974. The mineralogy, geochemistry and origin of lherzolite inclusions in Victorian basanites. Geochimica and Cosmochimica Acta 38, 1023-1050.

Frey, F.A., Prinz, D.H., 1978. Ultramafic inclusions from San Carlos volcanic field, Arizona: petrologic and geochemical data bearing on their petrogenesis. Earth and Planetary Sciece Letters 38, 129-176.

Galer, S.G.J., O'Nions, R.K., 1989. Chemical and isotopic studies of ultramafic inclusions from the San Carlos volcanic field, Arizona. Bearing on their petrogenesis. Journal of Petrology 30, 1033-1064.

Gregoire M., Moine B.M., O'Reilly S.Y., Cottin J.Y., Giret A. 2000. Trace element residence and partitioning in mantle xenoliths metasomatized by highly alkaline, silicate- and carbonate-rich melts (Kerguelen island, Indian Ovean). Journal of Petrology 41, 477-509.

Gudmundsson, O., Sambridge, M., 1998, A regionalized upper mantle (RUM) seismic model. Journal of Geophysical Research 103, B7121-7136.

Hart, S.R., Zindler, A., 1989. Constraints on the nature and the development of chemical heterogeneities in the mantle. In: W.R. Peltier (Editor), Mantle convection plate tectonics and global dynamics. New York: Gordon and Breach Sciences Publishers, pp. 261-388.

Hartmann, L.A., Leite, J. A. D., Da Silva, L. C., Remus, M. V. D., McNaughton, N. J., Groves, D. I., Fletcher, I. R., Santos, J. O. S., Vasconcellos, M. A. Z., 2000. Advances in SHRIMP geochronology and their impact on understanding the tectonic and metallogenic evolution of southern Brazil. Australian Journal of Earth Sciences 47: 829.

Hauri E.H., 1997. Melt migration and mantle chromatography, I: simplified theory and conditions for chemical and isotopic decoupling. Earth and Planetary Science Letters 153, 1-19.

Hauri, E.H., Shimizu, N., Dieu, J.J., Hart, S.R., 1993. Evidence of hot-spot related carbonatite metasomatism in the oceanic uppermantle. Nature 90, 297-314.

Hofmann, A.W., 1988. Chemical differentiation of the Earth: the relationship between mantle, continental crust and oceanic crust. Earth and Planetary Science Letters 153, 1-19.

Hofmann, A.W., 1997. Mantle chemistry: the message from oceanic volcanism. Nature 385, 219-228.

Johnson, K.T.M., Dick, H.J.B., Shimizu, N., 1990. Melting in oceanic upper mantle: an ion microprobe study of diopsides in abyssal peridotites. Journal Geophys. Res. 95, 2661-2678.

Keller, J., Hoefs, J. 1995. Stable isotope characteristics of recent natrocarbonatites from Oldoinyo Lengai. In: K. Bell and J. Keller (Editors), Carbonatite volcanism: Oldoynio Lengai and the petrogenesis of natrocarbonatites. Berlin, Springer, pp. 113-123.

Kyser, T.K., 1990. Stable isotopes in the continental lithospheric mantle. In: M.A. Menzies (Editor) Continental mantle. Oxford: Clarendon Press, pp. 127-156.

Kyser, T.K., O'Neil, J.R., Carmichael, I.S.E., 1981. Oxygen isotope thermometry of basic lavas and mantle nodules. Contributions to Mineralogy and Petrology 77, 11-23.

Laux, J.H., Pimentel M.M., Dantas, E.L., Armstrong, R., Junges, S.L., 2005, Two Neoproterozoic crustal accretion events in the Brasilia belt, central Brazil. Journal of South American Earth Sciences 18, 183-198.

Le Maitre, R.W., 1989. A classification of igneous rocks and glossary of terms. Oxford: Blackwell Scientific Publications, 193p.

Laurora, A., Mazzucchelli, M., Rivalenti, G., >Vannucci, R., Zanetti, A., Barbieri, M.A., Cingolani, C.A. 2001. Metasomatism and melting in carbonated peridotite xenoliths frm the mantle wedge: the Gobernador Gregore case (Southern Patagonia). Journal of Petrology 42, 69-87.

Liu, H.K., Gao, S.S., Silver, P.G., Zhang, Y., 2003. Mantle layering across central South America. Journal of Geophysical Research 108, B11, 2510.

Lucassen, F., Becchio, R., Wilke, H.G., Thirlwall, M.F., Viramonte, J., Franz, G., Wemmer, K., 2000. Proterozoic-Paleozoic development of the basement of the Central Andes (18°-26°) – a mobile belt of the South American craton. Journal of South American Earth Sciences 13, 697-715.

Lucassen, F., Escayola, M., Franz, G., Romer, R.L., Koch, K., 2002. Isotopic composition of late Mesozoic basic and ultrabasic rocks from Andes , 23-32º S) – implications for the Andean mantle. Contributions to Mineralogy and Petrology 143, 336-349.

Lucassen, F., Franz, G., Viramonte, J., Romer, R.L., Dulski P., Lang, A., 2005. The late Cretaceous lithospheric mantle beneath the Central Andes: evidence from phase equilibrium and composition of mantle xenoliths. Lithos 82, 379-406.

Lucassen, F., Kramer, W., Bartsch, V., Wilke, H-G., Franz, G., Romer, R.L., Dulski P., 2006. Nd, Pb and Sr isotope composition of juvenile magmatism in the <Mesozoic large magmatic province of northern Chile (18-27°S): indications for a uniform subarc mantle. Contrib. Mineral. Petrol. 152, 571-589.

Lucassen, F., Franz, G., Romer, R.L., Schultz F., Dulski P., Wemmer, K., 2007. Pre-Cenozoic intra-plate magmatism along the Central Andes (17-34°S): Composition of the mantle at an active margin. Lithos, in press.

Luhr, J.F., Aranda-Gomes, J.J., 1997. Mexican peridotite xenoliths and tectonic terranes: correlations among vent, location, texture, temperature, pressure and Oxygen fugacity. Journal of Petrology 38, 1075-1112.

McKenzie, D., O'Nions, R.K., 1991. Partial melt distributions from inversion of rare earth element concentrations. Journal of Petrology 32, 1021-1091.

Marques, L.S., Dupré B., Piccirillo E.M., 1999. Mantle source compositions of the Paraná magmatic province , southern Brazil): evidence from trace element and Sr-Nd-Pb isotope geochemistry. Journal of Geodynamics 28, 439-458.

Mattey, D., Lowry, D., MacPherson, C., 1994. Oxygen isotope composition of mantle olivine. Earth and Planetary Science Letters 128, 231-241.

Menzies, M.A., Hawkesworth, C.J., 1987. Mantle Metasomatism. Academic Press, Geology Series, London, 453 p.

Menzies, M.A., Kempton, P., Dungan, M. 1985. Interaction of continental lithosphere and asthenospheric melts below the Geronimo volcanic field, Arizona. Journal of Petrology 26, 663-693.

Mercier, J.C., 1980. Single-pyroxene geothermometry and geobarometry. American Journal of Sciences 61, 603-615.

Nimis, P:, Ulmer, P., 1998. Clinopyroxene geobarometry of magmatic rocks, part 1. an expanded structural geobarometer for anhydrous and hydrous, basic and ultrabasic system. Contributions to Mineralogy and Petrology 133, 122-125.

O'Reilly, S.Y., Griffin, W.C., 1988. Mantle metasomatism beneath western Victoria, Australia. 1: Metasomatic processes in Cr diopside lherzolites. Geochimica et Cosmochimica Acta 52, 433-448.

Orué, D., Censi, P., Velázquez, J.C., Comin-Chiaramonti, P., 1990. Geotérmia en la Provincia de Asunción. Revista de la Universidád Nacionál de Asunción 2, 62-66.

Petrini, R., Comin-Chiaramonti, P., Vannucci, R: 1994. Evolution of the lithosphere beneath Eastern Paraguay: geochemical evidence from mantle xenoliths in the Asunción-Ñemby nephelinites. Mineralogica et Petrographica Acta 37, 247-259.

Prinvivalle, F:, Tirone, M., Comin-Chiaramonti, P:, 2000. Clinopyroxenes from metasomatized spinel-peridotite mantle xenoliths from Ñemby (Paraguay): crystal chemistry and petrological implications. Mineralogy and Petrology 70, 25-35.

Renne, P.R., Ernesto, M., Pacca, I.G., Coe, R.S., Glen, J.M., Prévot, M., Perrin, M., 1992. The age of Paraná flood volcanism, rifting of Gondwanaland, and Jurassic-Cretaceous boundary. Science 258, 975-979.

Rivalenti, G., Mazzucchelli, M., Girardi, V.A.V., Vannucci, R., Barbieri, M.A., Zanetti, A., Goldstein, S.L., 2000. Composition and processes of the mantle lithosphere in northeastern Brazil and Fernando de Noronha: evidence from mantle xenoliths. Contributions to Mineralogy and Petrology 138, 308-325.

Rivalenti, G., Vannucci, R., Rampone, E., Mazzucchelli, M., Piccardo G.B., Piccirillo, E.M., Bottazzi, P., Ottolini, L., 1996. Peridotite clinopyroxene chemistry reflects mantle processes rather than continental versus oceanic settings.

Roden, M.F., Frey, F.A., Francis, D.M., 1984. An example of consequent mantle metasomatism in peridotite inclusions from Nunivak Island, Alaska. Journal of Petrology 25, 546-577.

Salters, V.J.M., Shimizu, N., 1988. World-wide occurrence of HFSE-depleted mantle. Geochimica et Cosmochimica Acta 52, 2177-2182.

Schultz, F., Lehmann, B., Tawackoli, S., Rössling, R., Belyatsky, B., Dulski, P., 2004. Carbonatite diversity in the Central Andes: the Ayopaya alkaline province, Bolivia. Contrib. Mineral. Petrol. 148, 391–408.

Sen, G., Frey, F.A., Shimizu, N., Leeman, W.P., 1993. Evolution of the lithosphere beneath Oahu (Hawaii): Rare Earth element abundance in mantle xenoliths. Earth and Planetary Science Letters 119, 53-69.

Song, Y., Frey, F.A., 1989. Geochemistry of peridotite xenoliths in basalts from Hannuoba, eastern China: implications for subcontinental mantle heterogeneity. Gechimica et Cosmochimica Acta 53, 97-113.

Spera, F.J., 1984. Carbon ioxide in petrogenesis. III: role of volatiles in the ascent of alkaline-bearing magmas with special reference to xenolith-bearing mafic lavas. Contribution to Mineralogy and Petrology 88, 217-232.

Stein, M., Navon, O., Kessel, R., 1997. Chromatographic metasomatism of the Arabian—Nubian lithosphere. Earth and Planetary Science Letters, 152, Issue 75-91.

Stern, C.R., Saul, S., Skewes, M.A., Futa, K., 1989. Farnet peridotite xenoliths from Pali-Aike basalts of southernmost South America. In: Kimberlites and related rocks. Geol.Soc. Australia, Special Publication 14, “° Vol., 735-744.

Stosch, H-G., Lungmair, G.W., 1986. Trace elements and Sm-Nd isotope geochemistry of peridotite xenoliths from Eifel (West Germany) and their bearing on the evolution of subcontinental lithosphere. Earth and Planetary Science Letters 90, 281-298.

Stracke, A., Bizimis, M., Salters, V.j:M., 2003. Recycling oceanic crust: quantitative constraints. Geochem. Geophys. Geosyt. 4 (3).

Sun, S.S., McDonough, W.F., 1989. Chemical and isotopic systematics of oceanic basalts. In: D. Saunders and M.J. Norry (Editors), Magmatism in the ocean basins. Geological Society, Special Paper 42, 313-345.

Takazawa, E., Frey, F.A., Shimizu, N., Obata, M., Bodinier, J.L., 1992. Geochemical evidence for melt migration and reaction in the upper mantle. Nature 359, 55-58.

VanDecar, J.C., James, D., Assumpção, M., 1995, Seismic evidence for a fossil mantle plume beneath South America and implications for driving forces. Nature 378, 25-31.

Vannucci, R., Ottolini, L., Bottazzi, P., Downes, H., Dupuy, C:, 19994. INAA, IDSM, SIMS comparative investigations of clinopyroxenes from mantle xenoliths with different textures. Chemical Geology 118, 85-108.

Velázquez, V.F., Riccomini, C., Gomes, C.B., Brumatti, M., 2002. Magmatismo alcalino da Província Misiones, Paraguai Oriental: aspectos geoquímicos e tectônicos. 41º Congresso Brasileiro de Geologia, João Pessoa, Anais, p. 546.

Velázquez, V.F., Comin-Chiaramonti, P., Cundari, A., Gomes, C.B., Riccomini, C., 2006. Cretaceous Na-alkaline magmatism from Misiones province (Paraguay): relationships with the Paleogene Na-alkaline analogue from Asunción and geodynamic significance. Journal of Geology 114, 593-614.

Wang, J., Hattori, K.H., Kilian, R., Stern, C.R., 2007.Metasomatism of sub-arc peridotites below southermost South America: reduction of fO_2 by slab-melt Contributions to Mineralogy and Petrology 153, 607-624.

Wells, P.R.A., 1977. Pyroxene thermometry in simple and complex systems. Contributions to Mineralogy and Petrology 42, 109-121.

White, W.M., 1985. Sources of oceanic basalts: radiogenic isotope evidence. Geology 13, 115-118.

Wilshire, H.G., Shervais, J.W., 1975. Al-augite and Cr-diopside ultramafic xenoliths in basaltic rocks from western United States. Physics and Cemistry of the Earth 9, 257-272.

Zindler, A., Hart, S.R., 1986. Chemical geodynamics. Annual Review of Earth and Planetary Sciences 14,493-571.

CAPTIONS TO THE FIGURES

Fig. 1. A: Map of the studied regions (modified after Comin-Chiaramonti et al., 2007, Lucassen et al., 2007) showing contours (red lines) of the depth (km) of the subducting Nazca slab based on seismic data (Gudmundsson and Sambridge, 1998). Heavy lines (black) outline the Cretaceous rift systems. The hatched area roughly marks the extension of intense early Paleozoic reworking of Proterozoic material, but the exact border to the Brazilian Craton remains unknown (cf. Lucassen et al., 2000). Pink fields delineate inferred positions of major cratonic fragments below Phanerozoic cover (after Laux et al., 2005): AAB, Arequipa-Antofalla; AC, Amazon Craton; AB, Apa Block; PR, Paranapanema; LP, Rio de la Plata; PA, Pampia. Localities characterized by sodic alkaline magmatism, mantle xenoliths bearing: 1, Asunción; 2, Misiones; 3, Belén; 4, Las Conchas and Cadillal; 5, Finca del Rodeo; 6, Betanzos (data sources: Comin-Chiaramonti et al., 2007 and Lucassen et al., 2007).
B: Seismic tomography image of Liu et al. (2003) across a profile approximately at 24° Lat. S. Note that the low-velocity feature in the mantle to the East has been interpreted as a fossil mantle plume by VanDecar et al. (1995).

Fig. 2. Plot, following De la Roche's (1980, 1986) nomenclature, of the rock-types reported in Table 1. R_1=4Si-11(Na+K)-2(Fe+Ti), R_2=6Ca+2Mg+Al; 1, ankaratrite; 2, basanite; 3, alkali basalt; 4, nephelinite; 5, tephrite; 6, trachybasalt. The whole compositional fields for the Misiones (M, light grey) and Asunción (A, dark grey) are also shown. **Inset**: Na_2O vs K_2O (wt%) diagram. Data source: Velázquez et al. (2006) and therein references; Lucassen et al. (2007).

Fig. 3. A: Trace elements are. normalized to the primitive mantle (Sun and McDonough, 1989) for average compositions of the mafic alkaline rocks from theParaguay and Andes compared with the whole field of the Paraguay mafic (sodic) analogues. **B**: REE are normalized to chondrite (Boynton, 1984) Data source as in Fig. 2.
C, D, E: Isotopic mixing curves between HIMU and potassic magmas from Early Cretaceous potassic rocks (ECK, Eastern Paraguay), computed using the following isotopic composition: HIMU (St. Helena; Chaffey et al., 1989); $^{87}Sr/^{86}Sr$=0.70282, Sr=650, $^{143}Nd/^{144}Nd$=0.5130, Nd=40, $^{206}Pb/^{204}Pb$=20.73, $^{207}Pb/^{204}Pb$=15.77 and $^{208}Pb/^{204}Pb$=40.80, U=1.44, Th=3.88, Pb=4, μ=24.4, κ=2.78; ECK, A: $^{87}Sr/^{86}Sr$=0.7070, Sr=1300, $^{143}Nd/^{144}Nd$=0.5117, Nd=60, $^{206}Pb/^{204}Pb$=16.672, $^{207}Pb/^{204}Pb$=15.422, $^{208}Pb/^{204}Pb$=37.10, U=1.47, Th=6.38, Pb=2, μ=23.09, κ=4.80; ECK B: $^{87}Sr/^{86}Sr$=0.7070, Sr=1300, $^{143}Nd/^{144}Nd$=0.5117, Nd=60, $^{206}Pb/^{204}Pb$=16.945, $^{207}Pb/^{204}Pb$=15.434, $^{208}Pb/^{204}Pb$=37.369, U=2.40, Th=9.10, Pb=15, μ=9.8, κ=3.8. Crosses: 10% step of mixing. DMM, HIMU and EMI components after Hart and Zindler (1989). Crystalline basement as in Antonini et al., 2005. For comparison the Ayopaya carbonatite is plotted (Lucassen et al., 2007).

Fig. 4. A. (SiO_2 + Al_2O_3)/(FeO_t + MgO) vs CaO/(FeO_t + MgO) diagram (molar ratios) for bulk-rock compositions relative to the Paraguay xenoliths, LK (I), HK (II) and Andean (III) suites, respectively. Stars B, H and BE: pyrolite compositions (Bristow, 1984), primitive mantle (Hofmann, 1988) and Bulk Earth (McKenzie & O'Nions, 1991), respectively. Data sources: Demarchi et al. (1988) and Lucassen et al, (2005). **B**: variation of the modal cpx vs the modal cpx/opx ratio. The line indicates model variation trends induced by non-modal fractionation melting in a primitive mantle composition (cf. Rivalenti et al., 2000); thicks are at 4% melting intervals; MM, mantle mode after Rivalenti et al., 1996.

Fig. 5. **A** - $\delta^{18}O_{cpx}$ vs $\delta^{18}O_{ol}$; regression lines for LK and HK suites and equilibration line (Δ = 0), respectively, are shown.. **B** - $\Delta^{18}O_{cpx-ol}$ vs isotopic equilibration temperatures, T°C, calculated according to Kyser (1990); the grey field represents the clinopyroxene-olivine pairs from South America mantle xenoliths (Kyser, 1990). **C** - Clinopyroxene-olivine fractionation as a function of clinopyroxene intracrystalline temperatures (Mercier, 1980); *Chiba*: fractionation line from Chiba et al. (1989). The data relative to the O isotopic values (V-SMOW9 are also shown; data source Comin-Chiaramonti et al., 2001.

Fig. 6. Trace element patterns of clinopyroxenes from Ñemby xenoliths, normalized to the primitive mantle (Hofmann, 1988) subdivided following LK (Py, Paraguay; *An*, Andes) and HK (Py) typology (panels A to D: LK; panels E to G: HK) and content % of the clinopyroxenes. Cpx, clinopyroxene, Opx, orthopyroxene, GD: The patterns of glassy drops and glassy patches are also shown. PMCE: clinopyroxene trace element composition in primitive mantle (Hofmann, 1988; cf. Rivalenti et al., 1996). In panels D and F the clinopyroxene pattern in the residue from non-modal fractional melting (6%) of primitive mantle (Hofmann, 1988) is reported; fractional melting parameters and partitions coefficients, after Johnson et al. (1990) and Rivalenti et al. (1996), respectively. Data sources, as in Table 3.

Fig. 7. REE patterns of clinopyroxenes normalized to the primitive mantle (Hofmann, 1988), and REE normalized to chondrites (Boynton, 1984). Symbols and panels, as in Fig. 6.

Fig. 8. $^{87}Sr/^{86}Sr$ vs $^{143}Nd/^{144}Nd$ plot for Ñemby clinopyroxenes and host mantle xenoliths; for comparison the compositions of the cpx from NE Brazil (NEB) and Fernando de Noronha (FDN; Rivalenti et al., 2000), Patagonia (PAT; Stern et al. 1989, Barbieri et al., 1997) are also plotted. L, leaching solutions (Comin-Chiaramonti et al., 2001). A, Host lavas from Andes (Lucassen et al., 2007); P, host lavas from Paraguay (Comin-Chiaramonti and Gomes, 1996, 2005).

Fig. 9. Sr, Nd and Pb isotopic composition of clinopyroxene separates and two Paraguay mantle xenoliths (cf. Fig. 3). Grey field: host lavas. Data sources as in Table 5. Symbols as in Fig. 3.

CAPTIONS TO THE TABLES

Table 1. Averaged compositions (in brackets standard deviations) for the sodic alkaline rock-types from Eastern Paraguay and Central Andes. Numbers as in Fig. 1. Data sources: Comin-Chiaramonti et al. (2001), Velázquez et al. (2006), Lucassen et al. (2007). (Eu/Eu)* calculoated according to the chondritic values after Boynton , 1984.

Table 2. Averaged isotopic analyses, time integrated ratios. For comparison the Apoyaya data are shown (Schultz et al., 2004 and Lucassen et al., 2007). Other sources as in Table 1.

Table 3. Trace elements in pyroxenes (Max and min, maximun and minimun concentration) from Paraguay (A) and Andes (A) mantle xenolithys, LK and HK suites, respectively and for glassy drops in clinopyroxene and glassy patches in xenoliths.. Data sources: Petrini et al. (1994), Comin-Chiaramonti et al. (1992, 2001), Lucassen et al. (2005). Primordial mantle Normalized ratios, PM; chondrite normalized ratios, CH. Paraguay data, ion microprobe analyses (analytical methods in Petrini et al., 1994), Andes data, ICP-MS (analytical methods in Lucassen et al., 2007).

Table 4. Rb, Sr, Sm , Nd contents and measured, initial ratios for Sr and Nd isotope ratios, ordered for increasing content of clinopyroxene (Cpx%). Data sources: Petrini et al. (19994), Comin-Chiaramonti et al. (2001), Velásquez et al. (2006), Comin-Chiaramonti and Gomes (2005), Lucassen et al. (2005). For comparison, data relative to the Apoyaya carbonatite (as in Lucassen et al. 2007) are reported. The following notional ages were considered for in-situ decay (s. text): Paraguay, 128 Ma, Andes, 100 Ma, Ayopaya, 140 Ma. LK, HK, low- anf high K suites, respectively; MIS, misiones; ASU, Asunción; WR, whole rock, CPX, clinopyroxene, OPX, orthopyroxene; CARB, carbonatized peridotic xenoliths, PYROX, pyroxenithic xenoliths. TDM: calculation of model dates relative to a depleted reservoir, $^{143}Nd/^{144}Nd$ = 0.513114 and $^{147}Sm/^{144}Nd$ = 0.222; Faure, 1986) are presented for plausible solutions.

Table 5. U, Th, Pb abundances and Pb isotopic composition of Andean clinopyroxenes and Paraguay xenoliths. Data sources: Lucassen et al. (2005), Comin-Chiaramonti and Gomes (2005). Only specimens with available isotopic Sr-Nd initial ratios are reported (cf. Table 4).

Author Agreement

The authors are in agreement:

Piero Comin-Chiaramoni, E-mail: comin@univ.triedte.it
Fiedrich Lucassen, E-mail: lucassen@gfz-potsdam.de
Angelo De Min, E-mail: demin@univ.trieste.it
Celso B. Gomes, E-mail: cgomes@usp.br

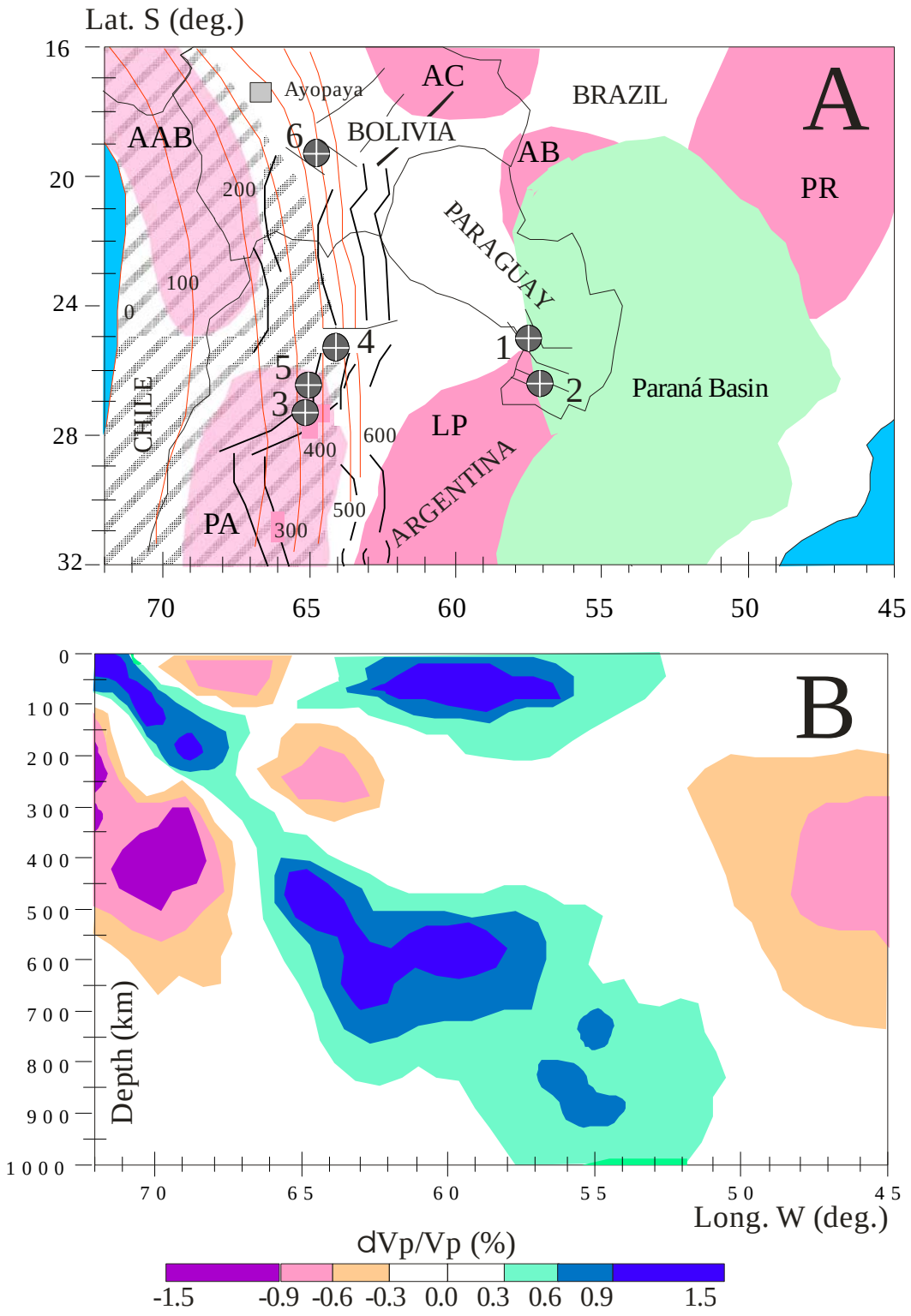
Lat. S (deg.)
16
20
24
28
32
70
65
60
55
50
45
A
Ayopaya
AC
BRAZIL
AAB
BOLIVIA
AB
PR
PARAGUAY
CHILE
LP
ARGENTINA
PA
Paraná Basin
0
100
200
300
400
500
600
1
2
3
4
5
6
B
Depth (km)
0
100
200
300
400
500
600
700
800
900
1000
Long. W (deg.)
dVp/Vp (%)
-1.5
-0.9
-0.6
-0.3
0.0
0.3
0.6
0.9
1.5

Fig.1

Fig.2.pdf

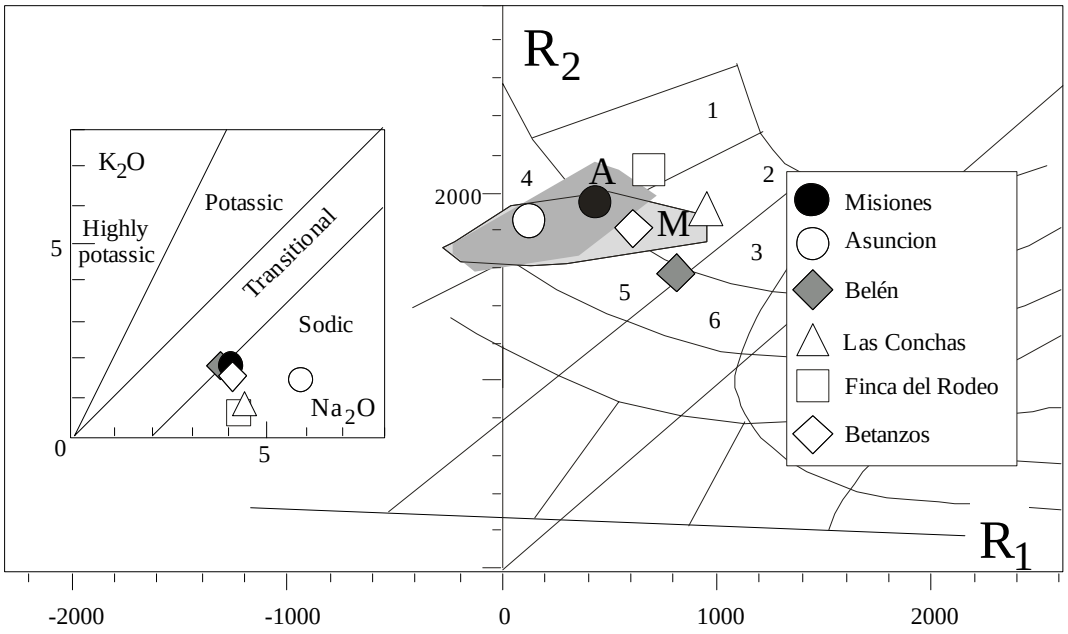

Fig. 2

Fig.3.pdf

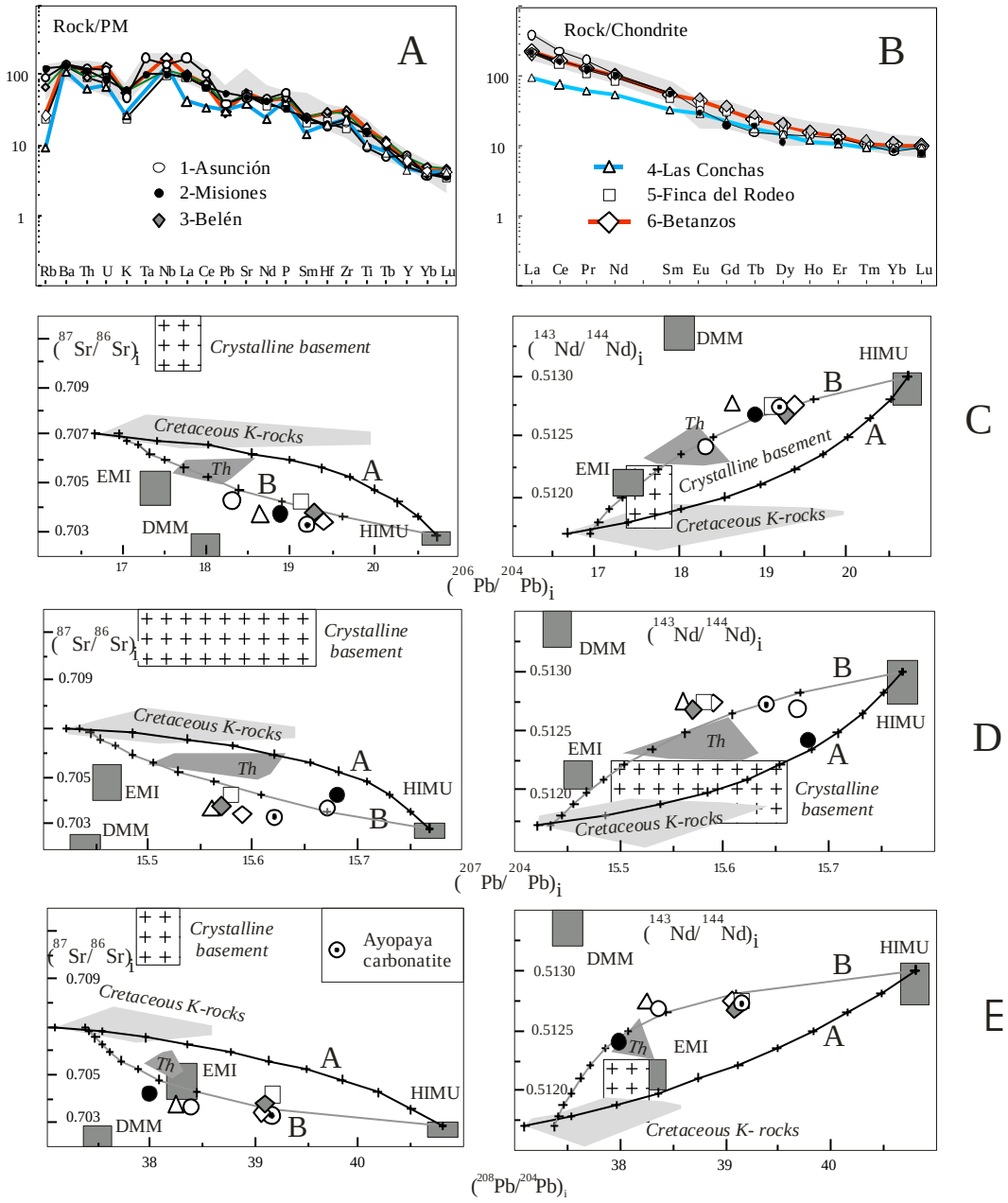

Fig. 3

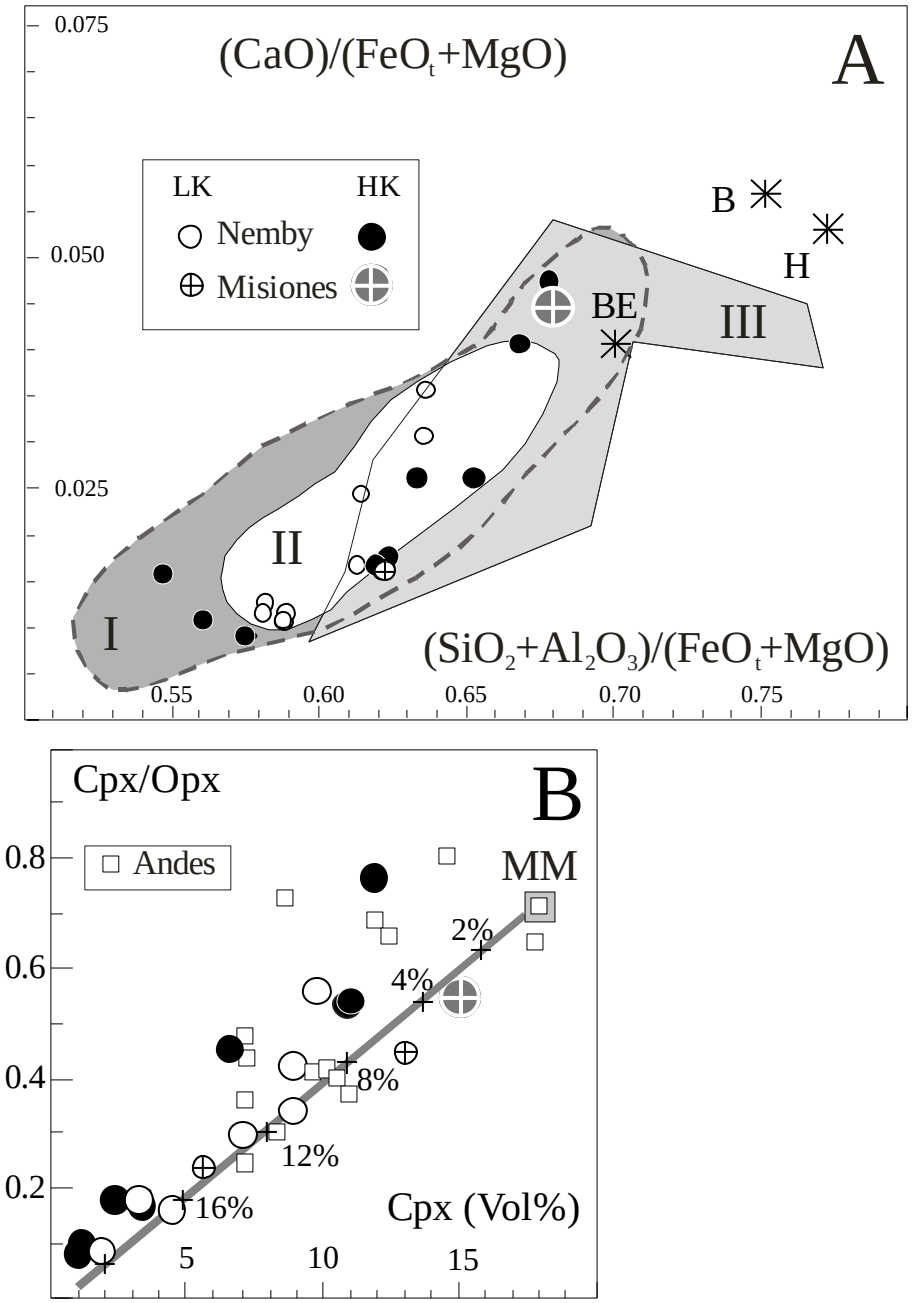
A
(CaO)/(FeOt+MgO)
0.075
0.050
0.025
LK
HK
Nemby
Misiones
B
H
BE
III
II
I
(SiO2+Al2O3)/(FeOt+MgO)
0.55
0.60
0.65
0.70
0.75
B
Cpx/Opx
Andes
MM
2%
4%
8%
12%
16%
Cpx (Vol%)
0.8
0.6
0.4
0.2
5
10
15

Fig. 4

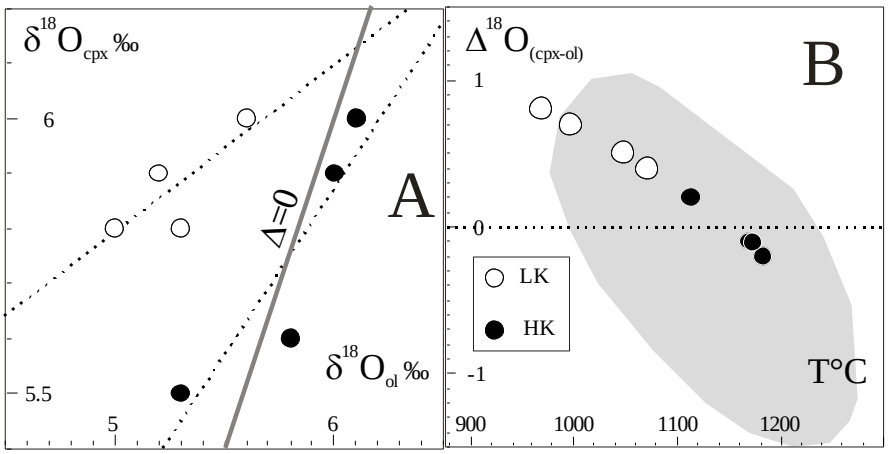

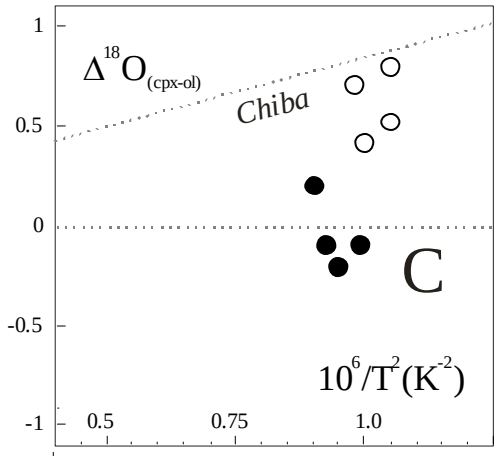

	LK				HK			
Sample	3192	3221	3227	3269	3331	3307	3211	3284
$\delta^{18}O‰_{Cpx}$	5.8	5.9	5.8	6.0	5.5	5.9	5.6	6.0
$\delta^{18}O‰_{Ol}$	5.0	5.2	5.3	5.6	5.3	6.0	5.8	6.1
T°C(K)	969	997	1048	1071	1113	1169	1183	1169
T°C(M)	976	1011	975	996	1053	1040	1025	1005

Fig. 5

Fig.6.pdf

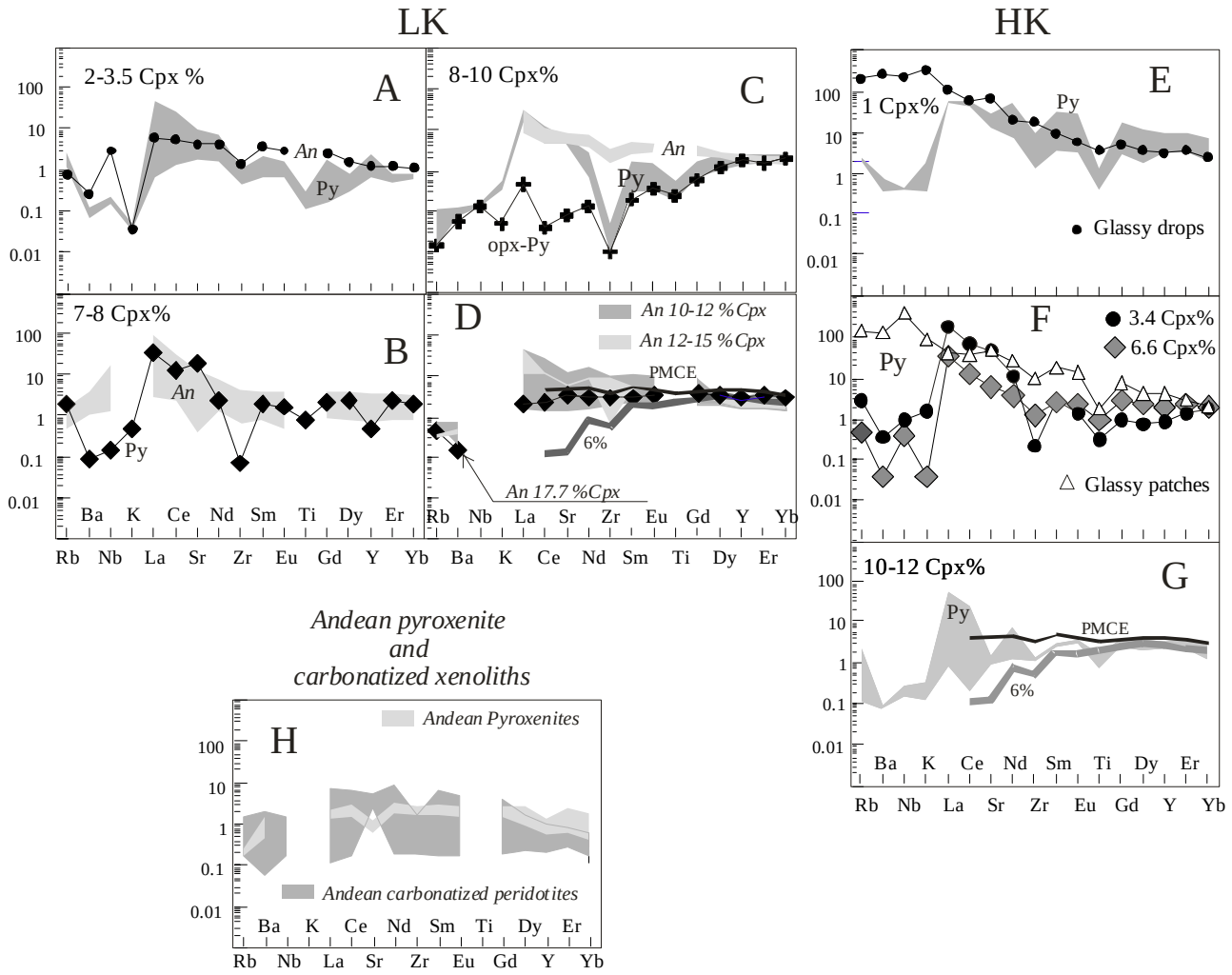

Fig. 6

Fig. 7.pdf

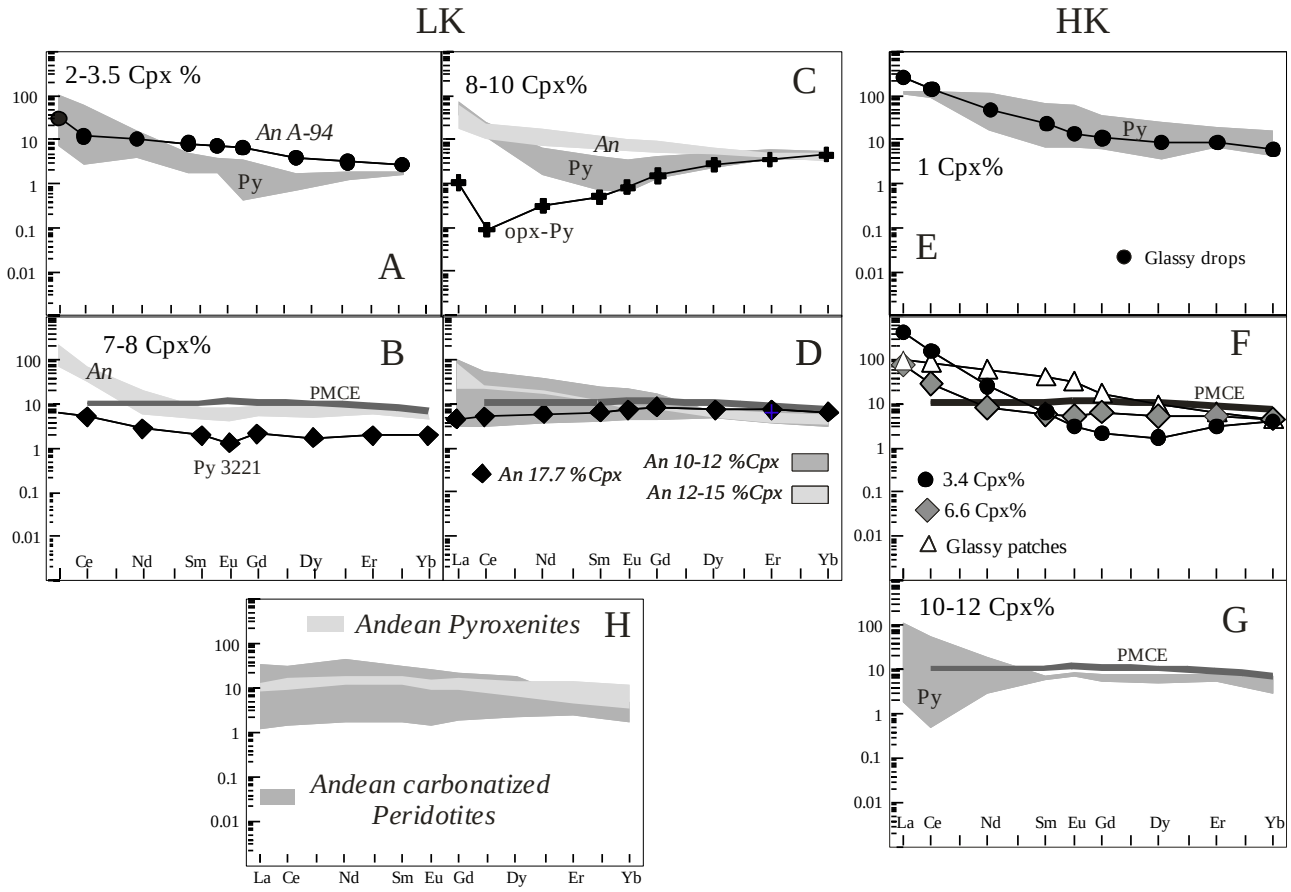

Fig. 7

Fig.8.pdf

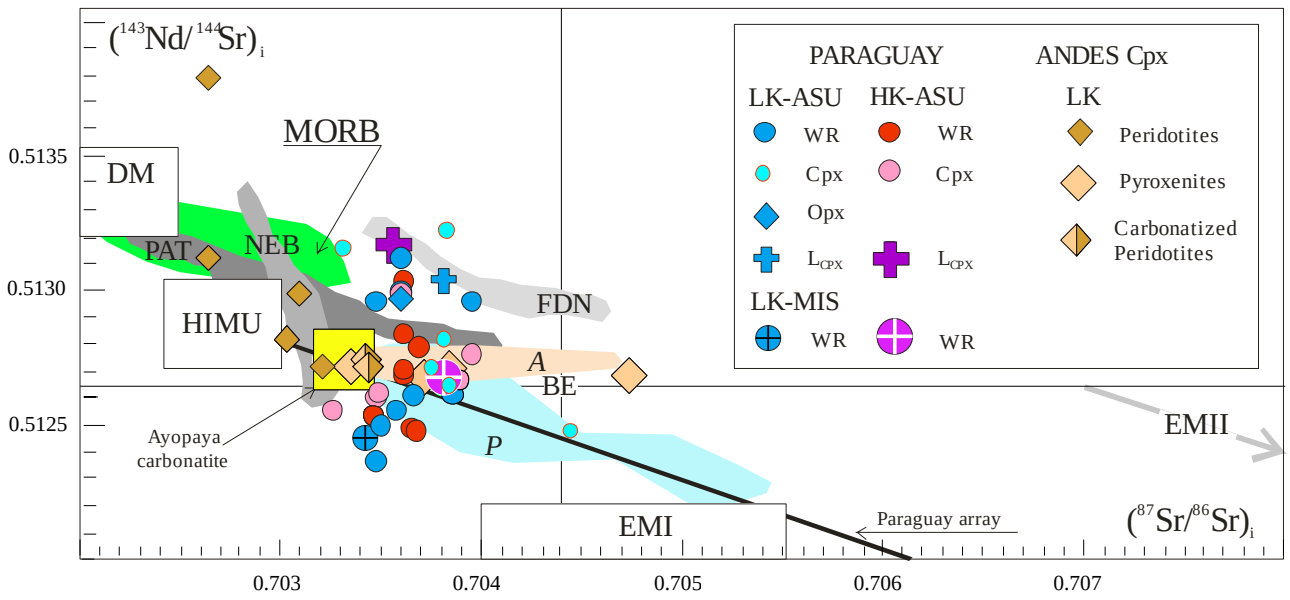

Fig. 8

Fig.9.pdf

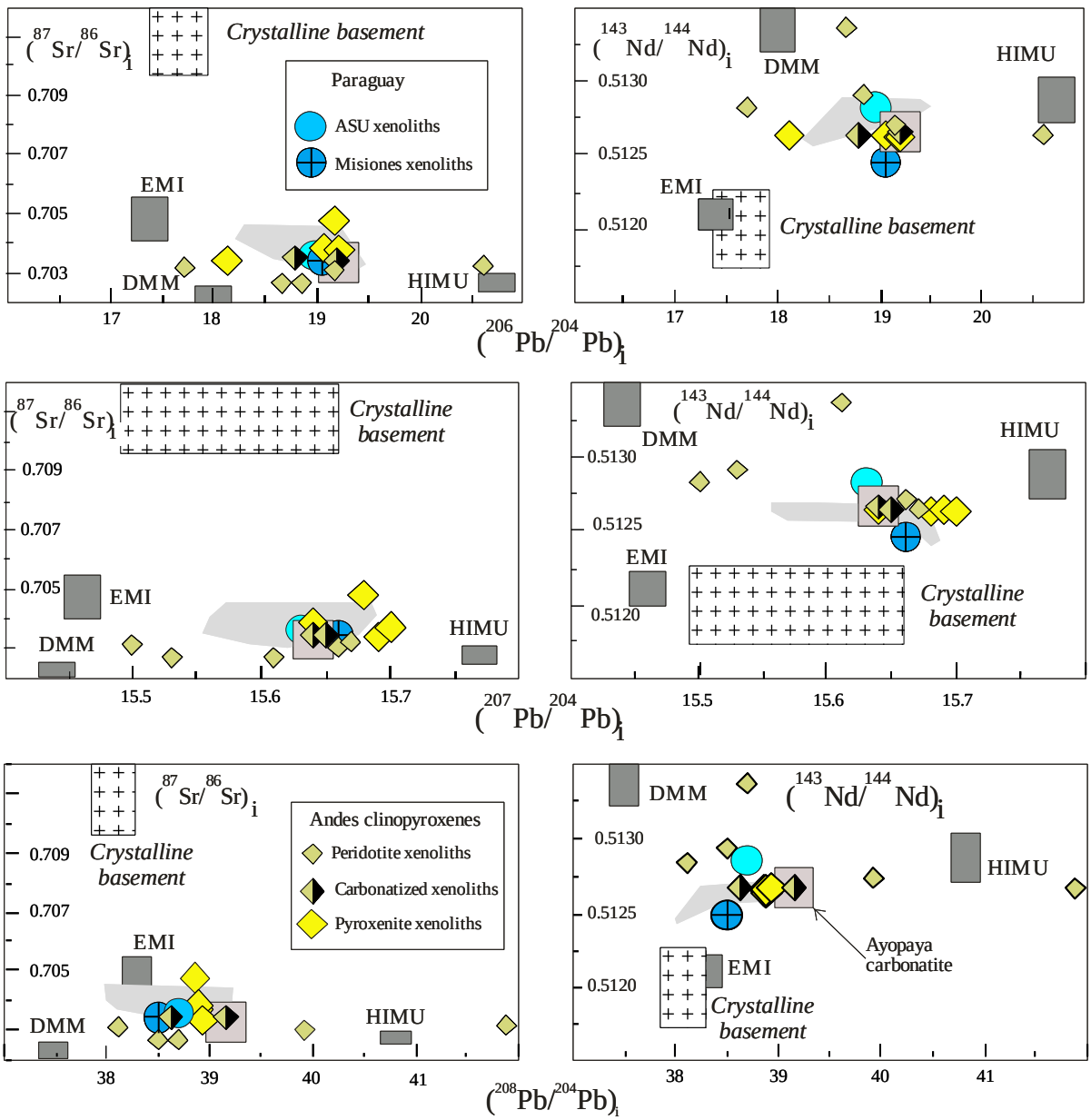

Fig. 9

Table 1

	1 ASUNCIÓN	2 MISIONES	3 BELÉN	4 LAS CONCHAS + CADILLAL	5 FINCA DEL RODEO	6 BETANZOS
Rock-type	melanephelinite	ankaratrite	tephrite	basanite	ankaratrite	basanite
N. of Samples	31	6	3	2	3	6
wt%						
SiO_2	42.91 (0.67)	41.43 (1.00)	44.70 (0.20)	45.25 (0.05)	41.53 (0.32)	43.35 (0.89)
TiO_2	2.05 (0.06)	3.50 (0.25)	4.10 (0.00)	2.20 (0.00)	3.20 (0.00)	3.77 (0.23)
Al_2O_3	13.41 (0.40)	13.07 (0.76)	14.63 (0.06)	14.75 (0.05)	13.60 (0.04)	13.90 (0.48)
FeO_{tot}	10.10 (0.60)	11.79 (0.29)	12.48 (0.35)	9.58 (0.05)	11.22 (0.07)	12.06 (0.49)
MnO	0.20 (0.02)	0.19 (0.01)	0.19 (0.02)	0.19 (0.00)	0.19 (0.01)	0.22 (0.03)
MgO	9.54 (0.51)	9.46 (0.58)	7.67(0.12)	10.50 (0.10)	10.97 (0.06)	8.12 (1.00)
CaO	10.45 (0.30)	11.46 (0.15)	8.40 (0.43)	10.35 (0.05)	12.33 (0.07)	10.57 (0.33)
Na_2O	5.80 (0.56)	4.88 (0.64)	3.67 (0.38)	4.35 (0.05)	4.27 (0.15)	4.10 (0.57)
K_2O	1.46 (0.39)	1.36 (0.24)	1.73 (0.21)	0.80 (0.00)	0.73 (0.12)	1.63 (0.23)
P_2O_5	1.18 (0.06)	0.74 (0.02)	1.03 (0.06)	0.93 (0.01)	0.78 (0.02)	0.97 (0.15)
LOI	2.19 (0.98)	1.84 (0.03)	–	–	–	–
Sum	98.89	99.72	98.60	99.77	98.82	98.69
Notional Age (Ma)	60	119	130	100	96	80
mg#	0.67	0.63	0.57	0.70	5.85	2.52
Na_2O/K_2O	3.97	3.59	2.12	5.44	0.67	0.59
ppm						
Cr	648 (65)	275 (34)	117 (30)	333 (13)	230 (10)	177 (99)
Ni	273 (15)	122 (6)	66 (12)	232 (6)	146 (2)	129 (77)
Rb	59 (9)	87.5 (11.9)	42 (16)	5.8 (2.3)	14.7 (29)	16.7 (5.4)
Ba	980 (87)	891 (62)	981 (233)	766 (15)	949 (31)	954 (76)
Th	11.0 (1.1)	7.11 (1.93)	7.88 (0.03)	5.32 (0.45)	7.78 (0.12)	9.56 (1.60)
U	2.4 (0.6)	1.47 (0.52)	2.12 (0.11)	1.45 (0.03)	1.58 (0.13)	2.73 (0.58)
Pb	10.3 (1.6)	7.31 (2.52)	7.26 (0.62)	5.55 (0.04)	7.06 (0.31)	5.47 (1.59)
Ta	7.1 (0.9)	4.0 (0.19)				
Nb	101 (7)	74 (2)	84 (1)	93 (1)	71 (0)	125 (17)
Sr	1013 (98)	1025 (70)	1097 (76)	798 (4)	1080 (174)	1147 (135)
Hf	5.5 (0.8)	6.24 (0.17)	9.36 (0.09)	5.94 (0.50)	6.58 (0.14)	8.60 (0.99)
Zr	234 (41)	270 (13)	321 (1)	256 (4.24)	190 (8)	341 (59)
Y	33 (3)	27 (4)	31.1 (1.5)	20.6 (0.6)	26.7 (0.4)	26.7 (2.8)
La	119 (7)	69.5 (13.9)	68.2 (0.6)	29.1 (0.6)	63.4 (1.1)	68.5 (22.8)
Ce	186 (11)	127 (26)	135.8 (2.4)	61.6 (1.1)	117.3 (2.8)	133.6 (37.5)
Pr	20.5 (3.2)	14.0 (2.9)	15.6 (0.4)	7.6 (0.0)	13.1 (0.3)	15.3 (3.7)
Nd	63.7 (5.1)	61.5 (7.2)	60.7 (1.8)	31.5 (0.1)	50.3 (0.7)	58.7 (11.8)
Sm	11.23 (2.98)	11.01 (1.44)	11.3 (0.5)	6.5 (0.1)	9.4 (0.3)	10.6 (1.5)
Eu	2.15 (0.57)	2.37 (0.07)	3.53 (0.12)	2.10 (0.00)	2.97 (0.06)	3.35 (0.22)
Gd	5.16 (1.37)	5.06 (0.66)	9.70 (0.52)	5.85 (0.21)	8.23 (0.15)	8.78 (1.07)
Tb	0.75 (0.20)	0.93 (0.15)	1.29 (0.03)	0.84 (0.01)	1.09 (0.01)	1.16 (0.12)
Dy	4.71 (1.67)	3.61 (0.47)	6.92 (0.29)	4.68 (0.04)	5.87 (0.05)	6.29 (0.58)
Ho			1.19 (0.06)	0.86 (0.01)	1.02 (0.02)	1.10 (0.11)
Er	2.75 (0.61)	2.30 (0.13)	3.13 (0.10)	2.25 (0.06)	2.60 (0.04)	2.81 (0.25)
Tm			0.40 (0.00)	0.30 (0.01)	0.32 (0.01)	0.35 (0.02)
Yb	1.79 (0.28)	1.78 (0.10)	2.42 (0.05)	1.97 (0.01)	1.91 (0.03)	2.17 (0.11)
Lu	0.30 (0.04)	0.25 (0.02)	0.35 (0.01)	0.30 (0.01)	0.26 (0.01)	0.31 (0.01)
(Eu/Eu)*	0.75	0.85	1.01	1.03	1.01	1.03

Table 2.

Location	Asunción	Misiones	Belén	Las Conchas and Cadillal	Finca del Rodeo	Betanzos	Ayopaya carbonatite
N. Samples	10	6	3	2	3	6	1
Notional Age	60	119	130	100	96	80	98
Rb	56±20	87.5±11.9	42±16	5.8±2.3	14.7±2.9	16.7±5.4	<0.1
Sr	1080±76	1025±70	1097±76	798±4	1080±174	1147±135	13440
$(^{87}Sr/^{86}Sr)i$	0.70367	0.70425	0.70380	0.70363	0.70418	0.70339	0.70329
±	0.00011	0.00016	0.00022	0.00004	0.00041	0.00022	0.00001
Sm	10.11±1.66	11.01±1.44	11.3±0.5	6.5±0.1	9.4±0.3	10.6±1.5	86.0
Nd	59.93±8.78	61.5±7.2	60.7±1.8	31.5±0.1	50.3±0.7	58.7±11.8	538.4
$(^{143}Nd/^{144}Nd)i$	0.51268	0.51242	0.51267	0.51275	0.51274	0.51274	0.51273
±	0.00006	0.00001	0.00001	0.00001	0.00001	0.00001	0.00001
ε Sr	-13.8	-4.5	-10.7	-13.5	-5.7	-17.2	-18.4
ε Nd	2.3	-1.2	3.8	4.7	4.3	4.3	4.3
U	2.00±0.03	1.47±0.52	2.12±0.11	1.45±0.01	1.58±0.13	2.73±0.58	3.48
Th	10.50±0.63	7.11±1.93	7.88±0.003	5.32±0.45	7.78±0.12	9.56±1.60	13.15
Pb	10.06±0.26	7.31±2.52	7.26±0.62	5.55±0.04	7.06±0.31	5.47±1.59	22.16
$(^{206}Pb/^{204}Pb)i$	18.89±0.07	18.31±0.14	19.29±0.08	18.63±0.00	19.13±0.01	19.39±0.17	19.20
$(^{207}Pb/^{204}Pb)i$	15.67±0.01	15.68±0.00	15.57±0.01	15.56±0.00	15.58±0.01	15.59±0.01	15.64
$(^{208}Pb/^{204}Pb)i$	38.37±0.17	37.97±0.01	39.09±0.07	38.25±0.05	39.16±0.02	39.06±0.18	39.15
μ	12. 8	12.8	19.1	16.8	14.6	25.5	10.2
κ	5.4	5.0	3.8	5.6	3.8	3.6	3.9

Tab. 3.

Suite	LK				LK				LK				LK		LK	
Cpx%	2-3%				7-8%				8-10%				10-12%		Pyroxenite	
Samples	P-3269; P-3227; P-M569X		A-94	P-3221	A-101; A-106; A-00179; A-6-18		P-3252; P-3254		P-3254	A-4-147; A-00177; A-6-178b		A-98d; A-6-179; A-7-169A; A-00175		A-4-233; A-4-240a; A-4-242; A-7-169b	
	Max	min			Max	min	Max	min	Opx	Max	min	Max	min	Max	min
ppm															
Rb	1.70	0.74	0.53	1.20	1.09	0.32	0.08	0.01	0.01			0.48	0.44	0.57	0.43
Ba	0.90	0.51	1.97	0.60	28.6	7.3	0.59	0.85	0.39	3.79	2.06	5.46	1.38	29.8	10.3
Nb	0.18	0.10	2.06	0.10	12.7	0.88	0.11	0.10	0.09	1.49	0.88	3.05	1.49		
K	12.50	8.50		118			142	90	11.4						
La	33.32	0.41	4.58	23.70	66.1	1.89	22.84	10.87	0.32	18.7	5.55	29.9	1.01	3.99	2.46
Ce	47.48	2.18	9.63	23.64	58.2	4.1	20.98	8.72	0.07	19	8.65	46.3	2.51	13.20	7.66
Sr	234	38	97.6	425	295	7.79	132	106	1.70	172	93.5	245	29.4	71.4	44.8
Nd	9.30	2.21	5.98	3.36	10.9	1.73	3.85	0.88	0.18	10.2	4.78	22.3	2.15	11.3	6.84
Zr	11.50	5.07	16	0.80	52	7.3	0.53	0.13	0.16	35.9	17	112	18.4	78.4	50.2
Sm	0.92	0.31	1.64	0.85	1.66	0.37	0.80	0.14	0.09	2.33	1.10	5.07	0.83	3.45	2.10
Eu	0.28	0.12	0.51	0.29	0.62	0.081	0.27	0.05	0.06	0.79	0.45	1.59	0.32	1.13	0.70
Ti	420	160		1065			750	260	314						
Gd	0.95	0.10	1.71	1.29	2.43	0.55	1.08	0.37	0.36	2.43	1.31	4.64	1.21	4.20	2.45
Dy	0.57	0.22	1.29	1.67	2.79	0.56	1.75	0.75	0.85	2.15	1.46	2.06	1.46	4.92	2.04
Y	11	3.20	5.9	2.30	15.1	3.27	12.0	6.20	7.50	10.8	6.68	13.4	6.83	17.50	8.44
Er	0.38	0.25	0.64	1.15	1.76	0.397	1.24	0.73	0.71	1.13	0.85	1.64	0.721	2.94	0.953
Yb	0.41	0.30	0.54	0.96	1.44	0.41	1.26	0.73	0.93	1.06	0.69	1.4	0.69	2.41	0.674
PM															
Sr/Sr*	*16.81*	*1.14*	*0.94*	*2.55*	*0.68*	*0.21*	*0.85*	*1.81*	*0.94*	*0.90*	*1.05*	*0.55*	*0.93*	*0.42*	*0.45*
Zr/Zr*	*0.23*	*0.39*	*0.35*	*0.03*	*0.79*	*0.62*	*0.02*	*0.02*	*0.06*	*0.61*	*0.51*	*0.72*	*0.89*	*0.87*	*0.97*
Ti/Ti*	*0.20*	*0.27*		*0.42*			*0.34*	*0.46*	*0.50*						
Y/Y*	*3.09*	*1.71*	*0.84*	*0.22*	*0.89*	*0.91*	*1.07*	*1.07*	*1.25*	*0.90*	*0.78*	*0.95*	*0.86*	*0.67*	*0.78*
CH															
(La/Sm)N	*22.78*	*1.03*	*1.76*	*17.53*	*25.05*	*3.21*	*17.96*	*48.83*	*2.24*	*5.05*	*3.17*	*3.71*	*0.77*	*0.73*	*0.74*
(Sm/Dy)N	*2.67*	*2.33*	*5.86*	*0.84*	*0.98*	*5.57*	*0.75*	*0.31*	*0.17*	*1.79*	*1.24*	*4.06*	*0.94*	*1.16*	*1.42*
(Gd/Yb)N	*1.87*	*0.27*	*2.56*	*1.08*	*1.36*	*1.08*	*0.69*	*0.41*	*0.31*	*1.85*	*1.53*	*2.67*	*1.42*	*1.41*	*2.93*
(La/Yb)N	*54.79*	*0.92*	*5.72*	*16.64*	*27.25*	*3.11*	*12.17*	*10.04*	*0.23*	*11.89*	*5.42*	*14.40*	*0.99*	*1.12*	*2.46*
(Eu/Eu)*	*0.91*	*1.65*	*0.92*	*0.85*	*0.94*	*0.62*	*0.89*	*0.63*	*0.89*	*1.01*	*1.14*	*0.98*	*0.97*	*0.91*	*0.94*

Tab. 3. (cont.)

Suite	LK		LK	LK		HK		HK	HK	HK		HK	HK
Cpx%	12-15%		17.7%	Carbonatized Peridotite		1%		3.4%	6.6%	10-12%		Glassy drops	Glassy patches
Samples	A-102; A-7-168b		A-104	A-57; A-113-c; A-4-229; A-4-301a		P-3284 P-SI-2A		P-3211	P-3307	P-3311; P-3222		P-3284	P-3211
	Max	min		Max	min	Max	min			Max	min		
ppm													
Rb	0.24	0.20	0.28	2.65	0.45	1.40	1.10	1.80	0.30	1.30	0.07	120	87
Ba	3.41	2.53	1.03	37.5	1.93	4.47	2.10	3.50	0.25	0.60	0.50	1781	823
Nb	8.6	6.4			0.49	0.30	0.25	0.70	0.30	0.20	0.11	155	277
K						3.81	81	397	10	90	30	82453	20091
La	28.12	7.09	1.36	10.7	0.36	38	323	119.4	23	36.14	0.58	77.39	29
Ce	20.6	19.9	3.95	25.5	1.16	98	68.4	121.5	22	45.55	0.38	106.25	68
Sr	119	110	70.1	268	132	525	248	977	130	336	18.4	1414	990
Nd	11.5	11	3.62	25.3	1.04	62	8.89	15.13	4.86	10.37	1.67	27.74	34
Zr	92.8	7.05	30.1	50.2	8.5	97	12.77	2.60	14	14.00	11.10	189	109
Sm	2.24	2.07	1.25	5.94	0.31	13.2	1.36	1.23	1.16	1.26	1.20	4.16	7.4
Eu	0.654	0.65	0.563	1.90	0.11	4.37	0.48	0.23	0.39	0.56	0.54	1.00	2.35
Ti						1482	4.83	405	1253	2157	955	4888	2338
Gd	2.21	1.88	2.12	5.35	0.46	9.71	1.56	0.56	1.60	2.02	1.45	2.92	4.70
Dy	2.29	1.46	2.40	3.31	0.67	7.8	1.14	0.55	1.54	2.58	1.63	2.61	3.18
Y	11.8	6.69	12.7	13.4	3.98	39	12.9	3.60	9.00	16.80	10.40	14.70	18.0
Er	1.38	0.75	1.54	1.19	0.49	3.95	1.36	0.69	1.12	1.63	1.10	1.68	1.29
Yb	1.24	0.67	1.35	1.02	0.33	3.24	0.90	0.82	0.96	1.38	0.60	1.23	0.98
PM													
Sr/Sr*	*0.56*	*0.54*	*1.36*	*0.77*	*8.86*	*0.49*	*0.52*	*1.16*	*0.77*	*0.10*	*1.21*	*1.67*	*1.48*
Zr/Zr*	*0.28*	*1.07*	*0.87*	*0.23*	*0.24*	*0.03*	*0.40*	*0.03*	*0.40*	*0.22*	*0.50*	*1.13*	*0.47*
Ti/Ti*				*0.05*	*0.14*	*0.27*	*0.38*	*0.27*	*0.38*	*0.49*	*0.26*	*0.69*	*0.16*
Y/Y*	*0.85*	*0.90*	*0.60*	*0.91*	*2.19*	*0.72*	*0.90*	*0.72*	*0.90*	*1.04*	*1.02*	*0.92*	*1.13*
CH													
(La/Sm)N	*1.13*	*0.73*	*0.73*	*1.81*	*14.95*	*61.01*	*12.47*	*61.01*	*12.47*	*18.05*	*0.30*	*11.72*	*2.47*
(Sm/Dy)N	*2.96*	*0.76*	*1.16*	*2.79*	*1.97*	*3.69*	*1.24*	*3.69*	*1.24*	*0.81*	*1.22*	*2.63*	*3.84*
(Gd/Yb)N	*4.23*	*1.13*	*1.41*	*2.43*	*1.41*	*0.55*	*1.39*	*0.55*	*1.39*	*1.18*	*1.95*	*1.91*	*3.87*
(La/Yb)N	*7.07*	*7,13*	*1.12*	*7.07*	*0.73*	*7.91*	*24.17*	*98.21*	*16.67*	*17.66*	*0.65*	*42.44*	*19.95*
(Eu/Eu)*	*1.01*	*0.89*	*0.91*	*1.13*	*1.01*	*0.74*	*0.88*	*0.74*	*0.88*	*1.07*	*1.25*	*0.83*	*1.14*

Tab. 4.

Suite/Sample	Cpx%	Rb	Sr	Sm	Nd	$(^{87}Sr/^{86}Sr)_m$	$(^{143}Nd/^{144}Nd)_m$	$(^{87}Sr/^{86}Sr)_i$	$(^{143}Nd/^{144}Nd)_i$	TDM Ma
LK										
MIS-WR										
PS-558B-MS	1.0	1.70	9.77	5.550	32.18	0.70438	0.51253	0.70343	0.51245	822
ASU-WR										
3269	1.9	1.74	9.94	0.010	0.29	0.70452	0.51267	0.70360	0.51265	371
3227	3.2	1.01	8.75	0.054	0.55	0.70446	0.51301	0.70385	0.51296	135
3253	3.5	0.65	8.98	0.036	0.20	0.70399	0.51305	0.70395	0.51296	140
3213	4.0	1.20	14.50	0.038	0.22	0.70392	0.51246	0.70348	0.51237	921
3199	4.5	1.92	16.94	0.012	0.20	0.70426	0.51264	0.70366	0.51261	427
3221	7.1	1.99	19.90	0.042	0.31	0.70410	0.51263	0.70357	0.51256	581
3252	8.9	0.70	6.12	0.040	0.150	0.70420	0.51311	0.70360	0.51300	109
3254	8.9	0.48	2.11	0.027	0.040	0.70480	0.51346	0.70360	0.51312	250
3192	9.8	1.07	6.80	0.040	0.25	0.70433	0.51258	0.70350	0.51250	713
ASU-OPX										
3252		-	-	0.030	0.18	0.70360	0.51305	0.70360	0.51297	131
ASU CPX										
3269		0.020	415.62	0.594	6.64	0.70444	0.51253	0.70444	0.51248	483
3227		0.022	199.43	0.469	4.80	0.70375	0.51277	0.70375	0.51272	364
3221		0.001	12.74	0.575	4.21	0.70384	0.51272	0.70384	0.51265	403
3254		1.45	9.80	0.089	0.18	0.70461	0.51348	0.70383	0.51322	627
3252		0.011	103.30	0.650	3.70	0.70382	0.51291	0.70382	0.51282	327
3192		0.136	45.85	2.595	4.71	0.70332	0.51344	0.70331	0.51316	386
*Leaching sol						0.70382	0.51304			
ANDES-CPX										
A-106	7.1	1.94	7.79	0.371	1.73	0.70368	0.51387	0.70264	0.51379	-
6-181	7.1	1.09	224	0.973	10.9	0.70323	0.51275	0.70321	0.51272	370
4-147-m	8.6	0.44	110	1.100	4.78	0.70304	0.51290	0.70303	0.51282	477
A-104	17.7	0.28	70.1	1.25	3.62	0.70312	0.51311	0.70310	0.51298	591
6-180a	26.1	0.68	39.2	0.948	2.85	0.70271	0.51325	0.70264	0.51312	-
CARB-L-CPX										
A-113e		0.45	223	2.69	13.70	0.70345	0.51280	0.70344	0.51272	535
4-301a		2.65	268	5.94	25.30	0.70346	0.51283	0.70342	0.51274	639
PYROX-CPX										
4-233		0.43	44.8	2.10	6.84	0.70339	0.51284	0.70335	0.51272	1411
4-240a		0.51	71.4	2.56	8.55	0.70374	0.51280	0.70371	0.51268	1496
4-242		0.57	62.7	2.18	7.35	0.70478	0.51281	0.70474	0.51269	1313
7-169b		0.49	54.9	3.45	11.30	0.70388	0.51283	0.70383	0.51271	1430
HK										
MIS-WR										
SI-2-A	1.0	4.25	40.77	1.36	8.89	0.70436	0.51276	0.70381	0.51268	473
ASU-WR										
3284	1.0	6.58	63.12	0.390	2.65	0.70401	0.51261	0.70346	0.51254	636
Leaching sol		120	1414	11.16	27.74	0.70401	0.51325	0.70380	0.51315	619
3220	1.1	0.59	14.22	0.076	0.56	0.70383	0.51276	0.70361	0.51269	436
3301	2.1	4.23	22.97	0.140	1.13	0.70464	0.51254	0.70367	0.51248	648
3313	2.4	3.93	58.02	0.210	2.42	0.70397	0.51288	0.70361	0.51284	249
3211	3.4	2.85	44.15	0.180	2.16	0.70380	0.51258	0.70346	0.51254	518
3307	6.6	0.05	28.20	0.190	2.05	0.70366	0.51254	0.70365	0.51249	573
3311	8.8	3.86	68.15	0.320	2.2	0.70399	0.51286	0.70369	0.51279	340
3222	10.9	1.38	14.33	0.470	1.12	0.70412	0.51325	0.70361	0.51304	434
3288	11.9	4.62	41.22	0.150	0.90	0.70420	0.51279	0.70361	0.51271	467
ASU CPX										
3284		1.73	653.79	16.145	84.34	0.70350	0.51272	0.70349	0.51262	638
3211		0.11	977.26	1.993	26.04	0.70326	0.51260	0.70326	0.51256	488
3307		0.04	173.74	0.841	4.13	0.70389	0.51277	0.70389	0.51267	607
3311		15.96	309.91	0.980	6.70	0.70422	0.51283	0.70395	0.51276	376
3222		0.12	44.8	0.873	2.40	0.70361	0.51317	0.70360	0.51299	-
3288		28.66	250.51	2.410	16.80	0.70408	0.51267	0.70348	0.51260	556
Ayopaya										
140		<0.1	13440	86.0	538.4	0.70329	0.51279	0.70329	0.51271	445

Table 5.

	U	Th	Pb	$(^{206}Pb/^{204}Pb)m$	$(^{207}Pb/^{204}Pb)m$	$(^{208}Pb/^{204}Pb)m$	μ	κ	$(^{206}Pb/^{204}Pb)i$	$(^{207}Pb/^{204}Pb)i$	$(^{208}Pb/^{204}Pb)i$
CPX											
A-104	0.028	0.03	0.39	17.78	15.5	38.13	4.5	1.1	17.71	15.50	38.11
A-106	0.242	1.02	6.83	18.70	15.61	38.74	2.4	4.4	18.66	15.61	38.69
A-147-m	0.180	0.07	0.22	20.02	15.66	40.04	55.0	0.4	19.16	15.66	39.93
6-180-a	0.089	0.33	1.82	18.89	15.53	38.56	3.1	3.8	18.84	15.53	38.50
6-181	0.368	1.40	3.42	20.73	15.68	42.03	7.4	3.9	20.61	15.67	41.89
CPX in carbonatized peridotites											
A-113e	0.087	0.05	0.95	18.87	15.65	38.79	6.0	0.6	18.78	15.65	38.62
4-301a	0.219	1.2	10.8	19.21	15.64	39.20	1.3	5.7	19.19	15.64	39.16
CPX in Pyroxenite											
4-233	0.074	0.29	5.9	18.13	15.65	38.96	0.7	4.5	18.12	15.69	38.94
4-240a	0.119	0.52	2.32	19.26	15.70	38.96	3.3	4.5	19.21	15.70	38.88
4-242	0.161	0.35	3.56	19.22	15.68	38.89	2.9	2.3	19.17	15.68	38.85
7-169b	0.066	0.26	1.34	19.11	15.64	38.94	3.2	4.1	19.06	15.64	38.88
ASU Xenolith (LK)											
3252				18.96	15.63	38.7					
MISIONES Xenolith (LK)											
PS-558B-X				19.05	15.66	38.50					